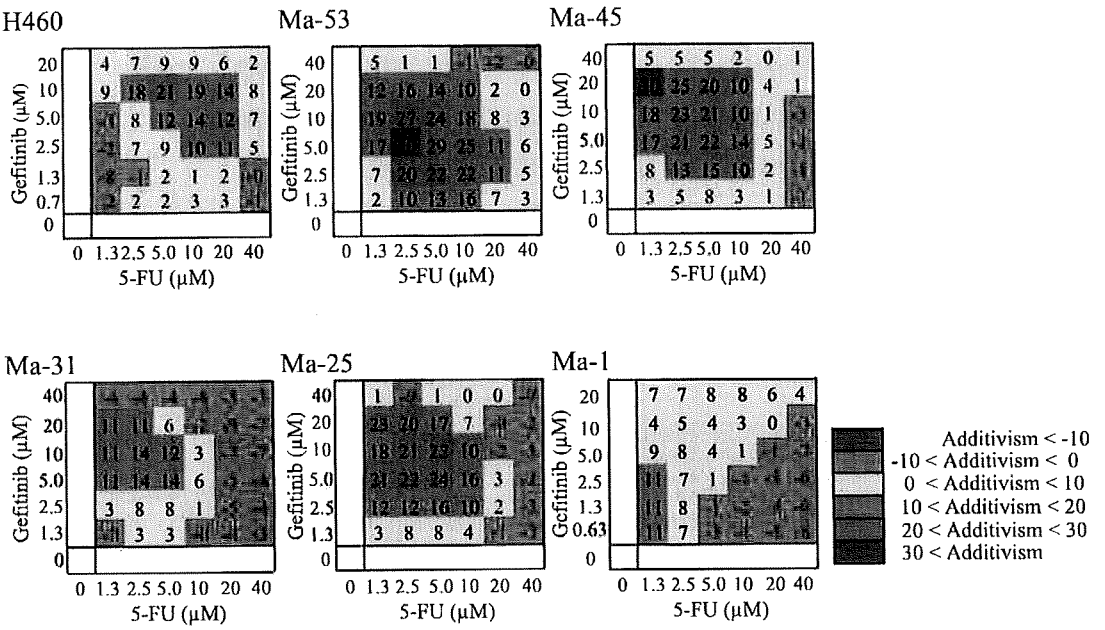

Figure 1. Inhibition of NSCLC cell growth by the combination of 5-FU and gefitinib *in vitro*. Cells with wild-type (H460, Ma-53, Ma-45, Ma-31, and Ma-25) or mutant (Ma-1) EGFR alleles were exposed for 72 h to 5-FU and gefitinib at the indicated concentrations, after which cell viability was measured with a colorimetric assay. The observed excess inhibition (%) relative to that predicted by the Bliss additivism model is shown color-coded in a drug concentration matrix for each cell line. Yellow, orange, pink, and red, synergy; light and dark blue, antagonism. Mean of triplicates from a representative experiment.

and *in vitro* in cells regardless of the absence or presence of *EGFR* mutations. Furthermore, we assessed the effects of gefitinib on the expression of enzymes that function in 5-FU metabolism, including thymidylate synthase (TS), DPD, and orotate phosphoribosyltransferase (OPRT), to gain insight into the mechanism underlying the synergistic effect of combination therapy with S-1 and gefitinib.

Materials and Methods

Cell Lines and Reagents

The human NSCLC cell lines NCI-H460 (H460), Ma-1, Ma-25, Ma-31, Ma-45, and Ma-53 were obtained as described previously (23). MiaPaca-2 cells were obtained from Japan Health Sciences Foundation. These cell lines were cultured under a humidified atmosphere of 5% CO_2 at 37°C in RPMI 1640 (Sigma) supplemented with 10% fetal bovine serum. Gefitinib was provided by AstraZeneca. S-1 and CDHP were provided by Taiho Pharmaceutical. 5-FU was obtained from Wako.

Growth Inhibition Assay *In vitro*

Cells (2.0×10^3) were plated in 96-well flat-bottomed plates and cultured for 24 h before the addition of various concentrations of 5-FU and gefitinib and incubation for an additional 72 h. Cell Counting Kit-8 solution (Dojindo) was then added to each well, and the cells were incubated for 3 h at 37°C before measurement of absorbance at 450 nm. Absorbance values were expressed as a percentage of that for untreated cells, and the concentration of 5-FU or gefitinib resulting in 50% growth inhibition (IC_{50}) was calculated. The effect of combining 5-FU and gefitinib was classified as additive, synergistic, or antagonistic with the Bliss additivism model (24–26). A theoretical curve was calculated for combined inhibition with the equation: $E_{bliss} = E_A + E_B - (E_A \times E_B)$, where E_A and E_B are the fractional inhibitory effects of drug A alone and drug B alone at specific concentrations. E_{bliss} is then the fractional inhibition that would be expected if the effect of the combination of the two drugs was exactly additive. In this study, the Bliss variable is expressed as percentage decrease in cell growth above what would be expected for the combination. Bliss = 0 indicates that the effect of the combination is additive; Bliss > 0 is indicative of synergy; and Bliss < 0 indicates antagonism.

Animals

Male athymic nude mice were exposed to a 12-h light, 12-h dark cycle and provided with food and water *ad libitum* in a barrier facility. All experiments were done in compliance with the regulations of the Animal Experimentation Committee of Taiho Pharmaceutical.

Growth Inhibition Assay *In vivo*

Cubic fragments of tumor tissue (~2 × 2 × 2 mm) were implanted s.c. into the axilla of 5- to 6-week-old male athymic nude mice. Treatment was initiated when tumors in each group achieved an average volume of 100 to 150 mm^3. Treatment groups consisted of control, S-1 alone, gefitinib alone, and the combination of S-1 and gefitinib. Each treatment group contained seven mice. S-1 (10 mg/kg body mass) and gefitinib (50 or 3 mg/kg) were administered by oral gavage once a day for 14 days; control animals

received 0.5% (w/v) hydroxypropylmethylcellulose as vehicle. Tumor volume was determined from caliper measurements of tumor length (L) and width (W) according to the formula LW^2 / 2. Both tumor size and body weight were measured two or three times per week.

Immunoblot Analysis

Cell lysates were fractionated by SDS-PAGE on 12% gels (NuPAGE Bis-Tris Gels; Invitrogen), and the separated proteins were transferred to a nitrocellulose membrane. After blocking of nonspecific sites with 5% skim milk, the membrane was incubated overnight at room temperature with primary antibodies. Antibodies to DPD, OPRT, and TS were obtained from Taiho Pharmaceutical; those to E2F-1 were from Santa Cruz Biotechnology; and those to β-actin (loading control) were from Sigma. Immune complexes were detected by incubation of the membrane for 1 h at room temperature with horseradish peroxidase–conjugated goat antibodies to mouse or rabbit immunoglobulin and by subsequent exposure to enhanced chemiluminescence reagents (Pierce).

Immunoprecipitation Analysis

Immunoprecipitation of EGFR was done according to standard procedures. Whole-cell lysates (800 μg protein) were incubated overnight at 4°C with antibodies to EGFR (Santa Cruz Biotechnology), after which Protein G Plus/Protein A-Agarose Suspension (Calbiochem) was added and the mixtures were incubated for an additional 1 h at 4°C. Immunoprecipitates were isolated, washed, resolved by SDS-PAGE on a 7.5% gel (Bio-Rad), and subjected to immunoblot analysis with antibodies to phosphotyrosine (PY20) and EGFR (Zymed).

Reverse Transcription and Real-time PCR Analysis

Total RNA (1 μg) extracted from cells with the use of an RNeasy Mini Kit (Qiagen) was subjected to reverse transcription with the use of a SuperScript Preamplification System (Invitrogen Life Technologies). The resulting cDNA was then subjected to real-time PCR analysis with the use of a TaqMan PCR Reagent Kit and a Gene Amp 5700 Sequence Detection System (Applied Biosystems). The forward and reverse primers and TaqMan probe for TS cDNA were 5-GCCTCGGTGTGCCTTTCA-3 and 5-CCCGTGATGTGCGCAAT-3 and 6-FAM-5′-TCGCCA-GCTACGCCCTGCTCA-3′-TAMRA, respectively. Glyceraldehyde-3-phosphate dehydrogenase mRNA were used as an internal standard.

Statistical Analysis

Data are presented as mean ± SE and were analyzed by the Aspin-Welch t test. $P < 0.05$ was considered statistically significant.

Results

Effect of the Combination of 5-FU and Gefitinib on NSCLC Cell Growth *In vitro*

Tegafur, which is a component of S-1, is metabolized to 5-FU in the liver and exerts antitumor effects. We first examined the antiproliferative activity of the combination of 5-FU and gefitinib in six NSCLC cell lines. Five of the cell lines (H460, Ma-53, Ma-45, Ma-31, and Ma-25) possess wild-type *EGFR* alleles, whereas Ma-1 cells harbor an *EGFR* mutation (E746_A750del) that is associated with a high response rate to the EGFR-TKIs gefitinib and erlotinib in individuals with advanced NSCLC. We assessed

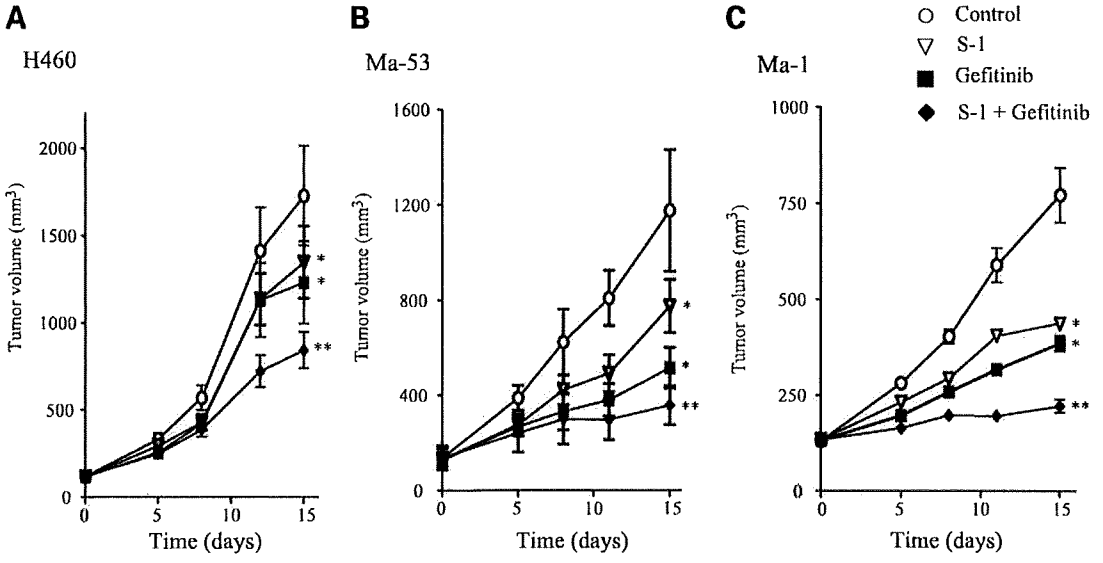

Figure 2. Antitumor activity of the combination of S-1 and gefitinib *in vivo*. **A** and **B**, nude mice with tumor xenografts established by s.c. implantation of NSCLC cells (H460 and Ma-53) possessing wild-type EGFR were treated daily for 2 wk with vehicle (control), S-1 (10 mg/kg), gefitinib (50 mg/kg), or both drugs by oral gavage. **C**, nude mice with tumor xenografts derived from NSCLC cells (Ma-1) expressing mutant EGFR were treated daily for 2 weeks with vehicle (control), S-1 (10 mg/kg), gefitinib (3 mg/kg), or both drugs by oral gavage. Tumor volume in all animals was determined at the indicated times after the onset of treatment. Mean ± SE of values from seven mice per group. *, $P < 0.05$ versus control; **, $P < 0.05$ versus S-1 or gefitinib alone for values 15 d after treatment onset (Aspin-Welch t test).

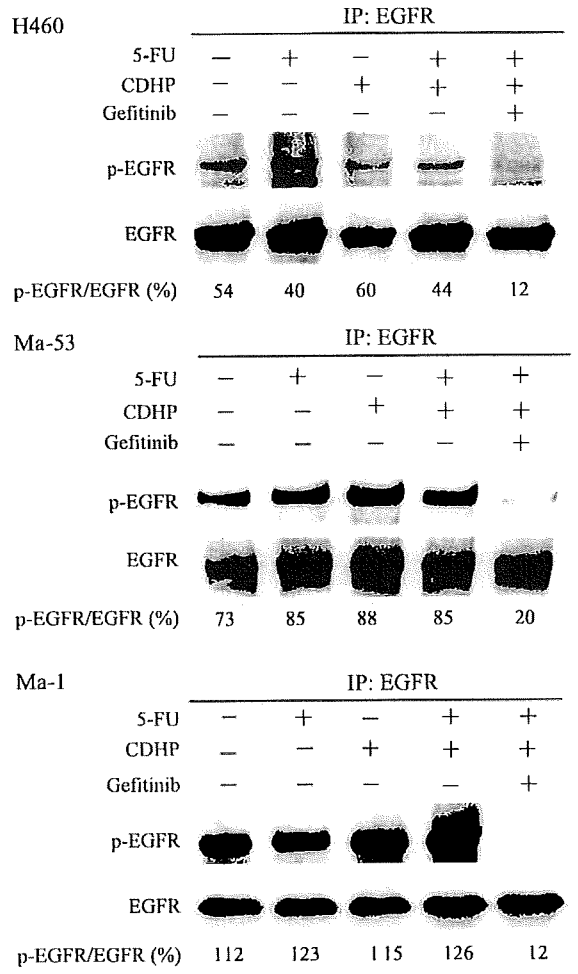

Figure 3. Lack of effect of 5-FU and CDHP on EGFR phosphorylation in NSCLC cell lines. NSCLC cells (H460, Ma-53, and Ma-1) were incubated for 24 h in medium supplemented with 2% fetal bovine serum and with 5-FU (10 μmol/L), CDHP (3 μmol/L), or gefitinib (5 μmol/L). Cell lysates were then prepared and subjected to immunoprecipitation (*IP*) with antibodies to EGFR, and the resulting precipitates were subjected to immunoblot analysis with antibodies to phosphotyrosine (for detection of phosphorylated EGFR) and with antibodies to EGFR. The intensity of the phosphorylated EGFR band relative to that of the EGFR band was determined by densitometry and is expressed as a percentage below each lane.

whether 5-FU and gefitinib showed additivity, synergy, or antagonism based on the Bliss additivism model (24–26). We chose this model rather than isobologram or combination index analysis because it would allow us to evaluate the nature of drug interactions even in instances in which the maximal inhibition by 5-FU or gefitinib alone was too low to obtain a reliable IC_{50} value. The six test concentrations for each agent were chosen after first determining the corresponding IC_{50} values. The IC_{50} values for 5-FU chemosensitivity were not associated with *EGFR* status and ranged from 7 to 11 μmol/L. The effect of combined treatment with 5-FU and gefitinib on the proliferation of the six NSCLC cell lines was tested in triplicate in a 6 × 6 concentration matrix. Calculation of the percentage inhibition in excess of that predicted by the Bliss additivism model revealed synergistic effects of Bliss > 0 for 5-FU and gefitinib in all of the six cell lines tested (Fig. 1). These results suggested that 5-FU and gefitinib act synergistically to inhibit cell growth in NSCLC cells.

Effect of Combined Treatment with S-1 and Gefitinib on NSCLC Cell Growth *In vivo*

We therefore next investigated whether combined treatment with S-1 and gefitinib might also exert a synergistic effect on NSCLC cell growth *in vivo*. Doses of both agents were selected so that their independent effects on tumor growth would be moderate. Nude mice were implanted s.c. with H460, Ma-53, or Ma-1 tumor fragments to establish tumor xenografts. When the H460 or Ma-53 tumors, which harbor wild-type *EGFR*, became palpable (100-150 mm^3), the mice were divided into four groups for daily treatment with vehicle, S-1 (10 mg/kg), gefitinib (50 mg/kg), or both drugs by oral gavage over 2 weeks. For xenografts formed by H460 or Ma-53 cells, combination therapy with S-1 and gefitinib resulted in a significant reduction in tumor size compared with that apparent in animals treated with S-1 or gefitinib alone (Fig. 2*A* and *B*). Mice bearing Ma-1 tumors, which express mutant *EGFR*, were treated with vehicle, S-1 (10 mg/kg), gefitinib (3 mg/kg), or both agents daily over 2 weeks. Combination treatment with S-1 and gefitinib significantly inhibited the growth of Ma-1 xenografts relative to that apparent in mice treated with either agent alone (Fig. 2C). None of the drug treatments induced a weight loss of >20% during the 2-week period, and no signs of overt drug toxicity were apparent (data not shown). These results thus suggested that combination chemotherapy with S-1 and gefitinib *in vivo* had a synergistic antitumor effect on NSCLC xenografts regardless of the absence or presence of *EGFR* mutations, consistent with our results *in vitro*.

Effects of 5-FU and CDHP on EGFR Phosphorylation in NSCLC Cell Lines

To investigate the mechanism responsible for the observed interaction between S-1 and gefitinib, we examined the effect of 5-FU on EGFR signal transduction in NSCLC cells expressing wild-type (H460 and Ma-53) or mutant (Ma-1) *EGFR*. Immunoprecipitation analysis revealed that exposure of H460 or Ma-53 cells to 5-FU (10 μmol/L) for 24 h had no effect on the basal level of EGFR phosphorylation (Fig. 3). We have shown previously that EGFR is constitutively phosphorylated in Ma-1 cells maintained in serum-free medium (23). Exposure of Ma-1 cells to 5-FU for 24 h did not affect this constitutive level of EGFR phosphorylation (Fig. 3). We next examined the effects of both CDHP, which is a component of S-1, and the combination of CDHP and 5-FU on EGFR phosphorylation in H460, Ma-53, and Ma-1 cells. Neither CDHP alone nor the combination of CDHP and 5-FU affected the level of EGFR phosphorylation in any of these three cell lines (Fig. 3). These results thus indicated that 5-FU and CDHP have no effect on EGFR signal transduction.

Effects of Gefitinib on the Expression of DPD, OPRT, and TS in NSCLC Cell Lines

We next investigated whether gefitinib might affect the expression of DPD, OPRT, or TS, enzymes that are major determinants of the sensitivity of cells to 5-FU. We first examined the abundance of these enzymes in the NSCLC cell lines H460, Ma-53, and Ma-1 by immunoblot analysis. The expression of DPD was detected in MiaPaca-2 cells (positive control) but not in H460, Ma-53, or Ma-1 cells (Fig. 4*A*). In contrast, OPRT and TS were detected in all three NSCLC cell lines and their abundance did not appear related to *EGFR* status (Fig. 4*A*). Treatment of H460, Ma-53, or Ma-1 cells with gefitinib (5 μmol/L) for up to 48 h resulted in a time-dependent decrease in the amount of TS, whereas that of OPRT or DPD remained unaffected (Fig. 4*B*). A reduced level of TS expression in tumors has been associated previously with a higher response rate to 5-FU-based chemotherapy (27, 28). Our data thus suggested that the suppression of TS expression by gefitinib might increase the sensitivity of NSCLC cells to 5-FU.

The transcription factor E2F-1 regulates expression of the TS gene (29–31). We therefore examined the possible effect of gefitinib on E2F-1 expression in NSCLC cell lines. Incubation of H460, Ma-53, or Ma-1 cells with gefitinib for up to 48 h also induced a time-dependent decrease in the amount of E2F-1 (Fig. 4*B*), suggesting that this effect might contribute to the down-regulation of TS expression by gefitinib in these cell lines.

Effect of Gefitinib on TS mRNA Abundance in NSCLC Cell Lines

The abundance of TS mRNA would be expected to be decreased if the down-regulation of E2F-1 expression by gefitinib was responsible for the reduced level of TS. We determined the amount of TS mRNA in H460, Ma-53, or Ma-1 cells at various times after exposure to gefitinib with the use of reverse transcription and real-time PCR analysis. Gefitinib indeed induced a time-dependent decrease in the amount of TS mRNA in all three NSCLC cell lines (Fig. 5), suggesting that the down-regulation of TS expression by gefitinib occurs at the transcriptional level and may be due to suppression of E2F-1 expression.

Discussion

The recent identification of activating somatic mutations of *EGFR* in NSCLC and their relevance to prediction of the therapeutic response to EGFR-TKIs such as gefitinib and erlotinib have had a major effect on NSCLC treatment (10–17). The response rate to these drugs remains low, however, in NSCLC patients with wild-tye *EGFR* alleles. Combination therapy with EGFR-TKIs and cytotoxic agents is a potential alternative strategy for NSCLC expressing wild-type *EGFR*. In the present study, we have evaluated the potential cooperative antiproliferative effect of combined treatment with the EGFR-TKI gefitinib and the new oral fluorouracil S-1 in NSCLC cell lines of differing *EGFR* status. We found that S-1 (or 5-FU) and gefitinib exert a synergistic antiproliferative effect on NSCLC cells both *in vivo* and *in vitro* regardless of the absence or presence of *EGFR* mutation. We chose a gefitinib dose of 50 mg/kg for treatment of mice bearing H460 or Ma-53 tumors. The median effective dose of gefitinib was shown previously to be ~50 mg/kg in athymic nude mice bearing A431 cell-derived xenografts (32). A gefitinib dose of 50 mg/kg has therefore subsequently been widely used in tumor xenograft studies (33–36). The U.S. Food and Drug Administration recommends that drug doses in animals be converted to those in humans based on body surface area (37). According to this guideline, a gefitinib dose of 50 mg/kg in mouse xenograft models is approximately equivalent to the therapeutic dose (250 mg/d) of the drug in humans. In addition, the tumor concentrations of gefitinib in NSCLC xenografts of mice treated with this drug (50 mg/kg) ranged from 9.7 to 13.3 μg/g, values that were similar to the

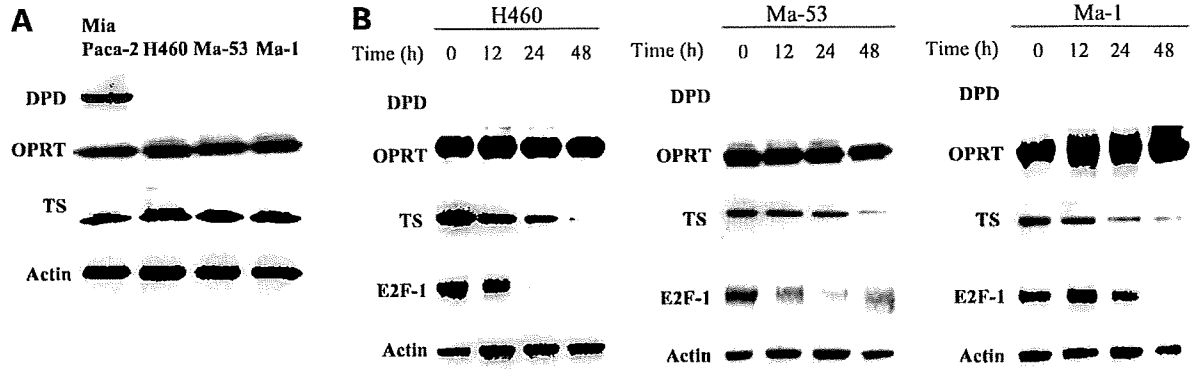

Figure 4. Effects of gefitinib on the expression of E2F-1, DPD, OPRT, and TS in NSCLC cell lines. **A**, lysates of H460, Ma-53, or Ma-1 cells were subjected to immunoblot analysis with antibodies to DPD, OPRT, TS, or β-actin (loading control). MiaPaca-2 cells were also examined as a positive control for DPD expression. **B**, NSCLC cells were incubated with gefitinib (5 μmol/L) for the indicated times in medium containing 10% serum, after which cell lysates were subjected to immunoblot analysis as in **A**, with the addition that E2F-1 expression was also examined.

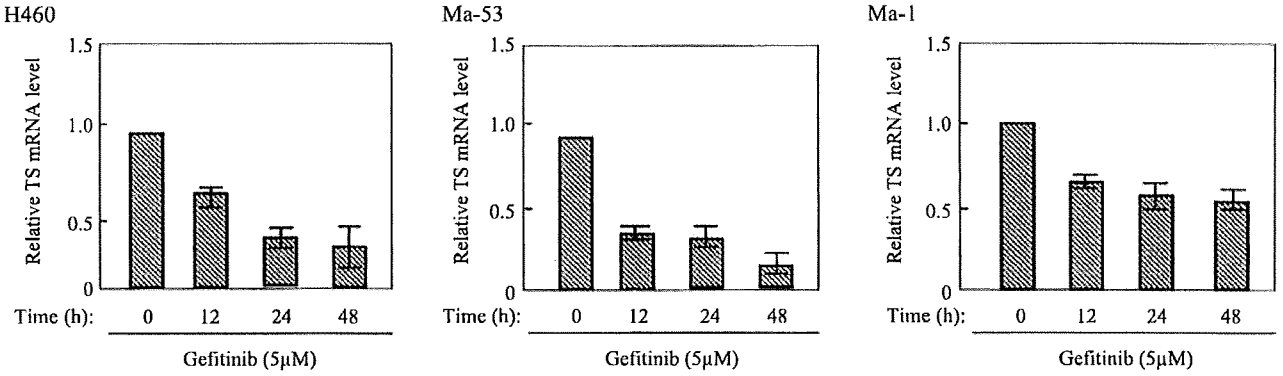

Figure 5. Down-regulation of TS mRNA by gefitinib in NSCLC cell lines. H460, Ma-53, or Ma-1 cells were incubated with gefitinib (5 μmol/L) for the indicated times in medium containing 10% serum, after which total RNA was extracted from the cells and subjected to reverse transcription and real-time PCR analysis of TS mRNA. The amount of TS mRNA was normalized by that of glyceraldehyde-3-phosphate dehydrogenase mRNA. Mean ± SE of values from three separate experiments.

achievable concentrations of gefitinib in tumor tissues of treated humans (34). These observations suggest that a gefitinib dose of 50 mg/kg in mouse xenograft models is appropriate for mimicking the therapeutic dose in humans.

EGFR-TKIs have been shown previously to act synergistically with radiation or cytotoxic agents such as cisplatin, paclitaxel, and irinotecan (38–40). These cytotoxic agents and radiation have been shown to increase the phosphorylation level of EGFR, possibly reflecting the activation of prosurvival signaling, and this effect is blocked by EGFR-TKIs, resulting in the synergistic antitumor effects of the combination therapies. Such a synergistic effect of 5-FU and gefitinib was attributed to 5-FU-induced EGFR phosphorylation in colorectal cancer cells (41). In contrast, we found that 5-FU had no effect on the level of EGFR phosphorylation in NSCLC cell lines. Further examination of different concentrations of 5-FU and different exposure times also failed to reveal an effect of 5-FU on EGFR phosphorylation in these cells (data not shown). These findings indicate that NSCLC cell lines respond differently to 5-FU than do colorectal cancer cells and that the synergistic antiproliferative effect of 5-FU and gefitinib in NSCLC cells is not mediated at the level of EGFR phosphorylation.

Our results indicate that the synergistic interaction of 5-FU (or S-1) and gefitinib is attributable, at least in part, to down-regulation of TS expression by gefitinib. The active metabolite of 5-FU, FdUMP, forms a covalent ternary complex with 5,10-methylenetetrahydrofolate and TS, resulting in inhibition of DNA synthesis (42). TS is thus an important therapeutic target of 5-FU. The amount of TS in neoplastic cells has been found to increase after exposure to 5-FU, resulting in the maintenance of free enzyme in excess of that bound to 5-FU (43–47). Such an increase in TS expression and activity has been viewed as a mechanistic driver of 5-FU resistance in cancer cells (48–50). The development of a new therapeutic strategy that reduces TS expression would therefore be of interest. Indeed, preclinical studies have shown that the down-regulation of TS by antisense oligonucleotides or other means enhances the efficacy of 5-FU (51–54). Down-regulation of TS would be expected to enhance the cytotoxicity of 5-FU as a result of the decrease in the amount of its protein target (55). Consistent with these preclinical data, an inverse relation between TS expression and 5-FU sensitivity has been shown in various human solid tumors (27, 28, 56–60). We have now shown that gefitinib alone induced down-regulation of TS expression, suggesting that this effect of gefitinib contributes to its synergistic interaction with 5-FU (or S-1) in NSCLC cell lines.

We further explored the molecular mechanism by which gefitinib induces down-regulation of TS expression in NSCLC cells. Given that EGFR signal transduction has been shown to be involved in activity of E2F-1 that regulates the expression of several genes including TS (61, 62), which controls the expression of several genes including that for TS, we examined the possible effects of gefitinib on E2F-1 expression and on the abundance of TS mRNA. Gefitinib induced down-regulation of E2F-1 in NSCLC cell lines harboring wild-type *EGFR*, consistent with previous observations (63), as well as in those expressing mutant *EGFR*. In addition, gefitinib reduced the amount of TS mRNA in NSCLC cells, consistent with the notion that the suppression of TS expression by gefitinib is attributable to inhibition of gene transcription as a result of down-regulation of E2F-1. For our experiments examining the effects of gefitinib on TS and E2F-1 expression, we used a drug concentration of 5 μmol/L. The concentration of gefitinib in tumor xenografts was shown previously to be 5 to 14 times that in the plasma concentration of the mouse hosts (34). Daily oral administration of gefitinib (250 mg) in patients also gave rise to a drug concentration in tumor tissue that was substantially higher (mean, 42-fold) than that in plasma concentration (34). We showed previously that the maximal concentration of gefitinib in the plasma of patients with advanced solid tumors had a mean value of 0.76 μmol/L at a daily dose of 225 mg (64). Based on these data, we considered that a gefitinib concentration of 5 μmol/L was appropriate for our

analyses of TS and E2F-1 expression. Together, our present findings suggest that down-regulation of E2F-1 and consequently that of TS by gefitinib is responsible, at least in part, for the synergistic antitumor effect of combined treatment with S-1 and gefitinib.

Somatic mutations of *EGFR* have been associated with sensitivity to EGFR-TKIs in patients with advanced NSCLC (13–16). However, although most NSCLCs with *EGFR* mutations initially respond to EGFR-TKIs, the vast majority of these tumors ultimately develop resistance to the drug. In the present study, the synergistic effect of combination chemotherapy with S-1 and gefitinib was observed even in *EGFR* mutant cells. Our findings thus suggest that the addition of S-1 (or 5-FU) to EGFR-TKIs might overcome chemoresistance to EGFR-TKIs and that exploration of the effect of such combination therapy in cells resistant to EGFR-TKIs is warranted. *EGFR* mutations appear to be largely limited to lung cancer, with few such mutations having been detected in other types of cancer (65–67). 5-FU is widely used as an anticancer agent and is considered a key drug in chemotherapy for solid tumors such as gastrointestinal and cervical cancer (68–70). Our present results show that gefitinib suppressed the expression of TS in NSCLC cell lines regardless of the absence or presence of *EGFR* mutations, suggesting that the addition of EGFR-TKIs to a 5-FU-containing regimen might increase the effectiveness of such treatment for solid cancers without *EGFR* mutations. Oral combined chemotherapy with drugs, such as S-1 and gefitinib, may also prove to be of low toxicity and therefore maintain quality of life. Our preclinical results provide a basis for future clinical investigations of combination chemotherapy with S-1 and EGFR-TKIs in patients with solid tumors.

References

1. Mendelsohn J, Baselga J. The EGF receptor family as targets for cancer therapy. Oncogene 2000;19:6550–65.
2. Schlessinger J. Cell signaling by receptor tyrosine kinases. Cell 2000; 103:211–25.
3. Hynes NE, Lane HA. ERBB receptors and cancer: the complexity of targeted inhibitors. Nat Rev Cancer 2005;5:341–54.
4. Hirsch FR, Varella-Garcia M, Bunn PA, Jr., et al. Epidermal growth factor receptor in non-small-cell lung carcinomas: correlation between gene copy number and protein expression and impact on prognosis. J Clin Oncol 2003;21:3798–807.
5. Suzuki S, Dobashi Y, Sakurai H, Nishikawa K, Hanawa M, Ooi A. Protein overexpression and gene amplification of epidermal growth factor receptor in nonsmall cell lung carcinomas. An immunohistochemical and fluorescence *in situ* hybridization study. Cancer 2005;103:1265–73.
6. Fukuoka M, Yano S, Giaccone G, et al. Multi-institutional randomized phase II trial of gefitinib for previously treated patients with advanced non-small-cell lung cancer (The IDEAL 1 Trial) [corrected]. J Clin Oncol 2003; 21:2237–46.
7. Perez-Soler R, Chachoua A, Hammond LA, et al. Determinants of tumor response and survival with erlotinib in patients with non-small-cell lung cancer. J Clin Oncol 2004;22:3238–47.
8. Thatcher N, Chang A, Parikh P, et al. Gefitinib plus best supportive care in previously treated patients with refractory advanced non-small-cell lung cancer: results from a randomised, placebo-controlled, multicentre study (Iressa Survival Evaluation in Lung Cancer). Lancet 2005;366:1527–37.
9. Shepherd FA, Rodrigues Pereira J, Ciuleanu T, et al. Erlotinib in previously treated non-small-cell lung cancer. N Engl J Med 2005;353: 123–32.
10. Lynch TJ, Bell DW, Sordella R, et al. Activating mutations in the epidermal growth factor receptor underlying responsiveness of non-small-cell lung cancer to gefitinib. N Engl J Med 2004;350:2129–39.
11. Paez JG, Janne PA, Lee JC, et al. EGFR mutations in lung cancer: correlation with clinical response to gefitinib therapy. Science 2004;304: 1497–500.
12. Pao W, Miller V, Zakowski M, et al. EGF receptor gene mutations are common in lung cancers from "never smokers" and are associated with sensitivity of tumors to gefitinib and erlotinib. Proc Natl Acad Sci U S A 2004;101:13306–11.
13. Mitsudomi T, Kosaka T, Endoh H, et al. Mutations of the epidermal growth factor receptor gene predict prolonged survival after gefitinib treatment in patients with non-small-cell lung cancer with postoperative recurrence. J Clin Oncol 2005;23:2513–20.
14. Takano T, Ohe Y, Sakamoto H, et al. Epidermal growth factor receptor gene mutations and increased copy numbers predict gefitinib sensitivity in patients with recurrent non-small-cell lung cancer. J Clin Oncol 2005;23: 6829–37.
15. Han SW, Kim TY, Hwang PG, et al. Predictive and prognostic impact of epidermal growth factor receptor mutation in non-small-cell lung cancer patients treated with gefitinib. J Clin Oncol 2005;23: 2493–501.
16. Tsao MS, Sakurada A, Cutz JC, et al. Erlotinib in lung cancer—molecular and clinical predictors of outcome. N Engl J Med 2005;353: 133–44.
17. Tokumo M, Toyooka S, Kiura K, et al. The relationship between epidermal growth factor receptor mutations and clinicopathologic features in non-small cell lung cancers. Clin Cancer Res 2005;11:1167–73.
18. Shirasaka T, Shimamoto Y, Fukushima M. Inhibition by oxonic acid of gastrointestinal toxicity of 5-fluorouracil without loss of its antitumor activity in rats. Cancer Res 1993;53:4004–9.
19. Tatsumi K, Fukushima M, Shirasaka T, Fujii S. Inhibitory effects of pyrimidine, barbituric acid and pyridine derivatives on 5-fluorouracil degradation in rat liver extracts. Jpn J Cancer Res 1987;78:748–55.
20. Shirasaka T, Shimamato Y, Ohshimo H, et al. Development of a novel form of an oral 5-fluorouracil derivative (S-1) directed to the potentiation of the tumor selective cytotoxicity of 5-fluorouracil by two biochemical modulators. Anticancer Drugs 1996;7:548–57.
21. Kawahara M, Furuse K, Segawa Y, et al. Phase II study of S-1, a novel oral fluorouracil, in advanced non-small-cell lung cancer. Br J Cancer 2001;85:939–43.
22. Ichinose Y, Yoshimori K, Sakai H, et al. S-1 plus cisplatin combination chemotherapy in patients with advanced non-small cell lung cancer: a multi-institutional phase II trial. Clin Cancer Res 2004;10:7860–4.
23. Okabe T, Okamoto I, Tamura K, et al. Differential constitutive activation of the epidermal growth factor receptor in non-small cell lung cancer cells bearing EGFR gene mutation and amplification. Cancer Res 2007;67:2046–53.
24. Berenbaum MC. Criteria for analyzing interactions between biologically active agents. Adv Cancer Res 1981;35:269–335.
25. Borisy AA, Elliott PJ, Hurst NW, et al. Systematic discovery of multicomponent therapeutics. Proc Natl Acad Sci U S A 2003;100:7977–82. Epub 2003 Jun 10.
26. Buck E, Eyzaguirre A, Brown E, et al. Rapamycin synergizes with the epidermal growth factor receptor inhibitor erlotinib in non-small-cell lung, pancreatic, colon, and breast tumors. Mol Cancer Ther 2006;5:2676–84.
27. Ichikawa W, Uetake H, Shirota Y, et al. Combination of dihydropyrimidine dehydrogenase and thymidylate synthase gene expressions in primary tumors as predictive parameters for the efficacy of fluoropyrimidine-based chemotherapy for metastatic colorectal cancer. Clin Cancer Res 2003;9:786–91.
28. Salonga D, Danenberg KD, Johnson M, et al. Colorectal tumors responding to 5-fluorouracil have low gene expression levels of dihydropyrimidine dehydrogenase, thymidylate synthase, and thymidine phosphorylase. Clin Cancer Res 2000;6:1322–7.
29. DeGregori J, Kowalik T, Nevins JR. Cellular targets for activation by the E2F1 transcription factor include DNA synthesis- and G_1/S-regulatory genes. Mol Cell Biol 1995;15:4215–24.
30. Dyson N. The regulation of E2F by pRB-family proteins. Genes Dev 1998;12:2245–62.
31. Trimarchi JM, Lees JA. Sibling rivalry in the E2F family. Nat Rev Mol Cell Biol 2002;3:11–20.

32. Wakeling AE, Guy SP, Woodburn JR, et al. ZD1839 (Iressa): an orally active inhibitor of epidermal growth factor signaling with potential for cancer therapy. Cancer Res 2002;62:5749 – 54.

33. Matar P, Rojo F, Cassia R, et al. Combined epidermal growth factor receptor targeting with the tyrosine kinase inhibitor gefitinib (ZD1839) and the monoclonal antibody cetuximab (IMC-C225): superiority over single-agent receptor targeting. Clin Cancer Res 2004;10:6487 – 501.

34. McKillop D, Partridge EA, Kemp JV, et al. Tumor penetration of gefitinib (Iressa), an epidermal growth factor receptor tyrosine kinase inhibitor. Mol Cancer Ther 2005;4:641 – 9.

35. Zhang X, Chen ZG, Choe MS, et al. Tumor growth inhibition by simultaneously blocking epidermal growth factor receptor and cyclo-oxygenase-2 in a xenograft model. Clin Cancer Res 2005;11:6261 – 9.

36. Haura EB, Zheng Z, Song L, Cantor A, Bepler G. Activated epidermal growth factor receptor-Stat-3 signaling promotes tumor survival *in vivo* in non-small cell lung cancer. Clin Cancer Res 2005;11:8288 – 94.

37. U S. Department of Health and Human Services, Food and Drug Administration, Center for Drug Evaluation and Research (CDER). Guidance for industry, estimating the maximum safe starting dose in initial clinical trials for therapeutics in adult healthy volunteers; 2005. p. 1 – 27.

38. Koizumi F, Kanzawa F, Ueda Y, et al. Synergistic interaction between the EGFR tyrosine kinase inhibitor gefitinib ("Iressa") and the DNA topoisomerase I inhibitor CPT-11 (irinotecan) in human colorectal cancer cells. Int J Cancer 2004;108:464 – 72.

39. Chinnaiyan P, Huang S, Vallabhaneni G, et al. Mechanisms of enhanced radiation response following epidermal growth factor receptor signaling inhibition by erlotinib (Tarceva). Cancer Res 2005;65:3328 – 35.

40. Van Schaeybroeck S, Kyula J, Kelly DM, et al. Chemotherapy-induced epidermal growth factor receptor activation determines response to combined gefitinib/chemotherapy treatment in non-small cell lung cancer cells. Mol Cancer Ther 2006;5:1154 – 65.

41. Van Schaeybroeck S, Karaiskou-McCaul A, Kelly D, et al. Epidermal growth factor receptor activity determines response of colorectal cancer cells to gefitinib alone and in combination with chemotherapy. Clin Cancer Res 2005;11:7480 – 9.

42. Peters GJ, van der Wilt CL, van Triest B, et al. Thymidylate synthase and drug resistance. Eur J Cancer 1995;31A:1299 – 305.

43. Spears CP, Shahinian AH, Moran RG, Heidelberger C, Corbett TH. *In vivo* kinetics of thymidylate synthetase inhibition of 5-fluorouracil-sensitive and -resistant murine colon adenocarcinomas. Cancer Res 1982;42:450 – 6.

44. Washtien WL. Increased levels of thymidylate synthetase in cells exposed to 5-fluorouracil. Mol Pharmacol 1984;25:171 – 7.

45. Spears CP, Gustavsson BG, Berne M, Frosing R, Bernstein L, Hayes AA. Mechanisms of innate resistance to thymidylate synthase inhibition after 5-fluorouracil. Cancer Res 1988;48:5894 – 900.

46. Swain SM, Lippman ME, Egan EF, Drake JC, Steinberg SM, Allegra CJ. Fluorouracil and high-dose leucovorin in previously treated patients with metastatic breast cancer. J Clin Oncol 1989;7:890 – 9.

47. Chu E, Zinn S, Boarman D, Allegra CJ. Interaction of γ interferon and 5-fluorouracil in the H630 human colon carcinoma cell line. Cancer Res 1990;50:5834 – 40.

48. Johnston PG, Drake JC, Trepel J, Allegra CJ. Immunological quantitation of thymidylate synthase using the monoclonal antibody TS 106 in 5-fluorouracil-sensitive and -resistant human cancer cell lines. Cancer Res 1992;52:4306 – 12.

49. Copur S, Aiba K, Drake JC, Allegra CJ, Chu E. Thymidylate synthase gene amplification in human colon cancer cell lines resistant to 5-fluorouracil. Biochem Pharmacol 1995;49:1419 – 26.

50. Kawate H, Landis DM, Loeb LA. Distribution of mutations in human thymidylate synthase yielding resistance to 5-fluorodeoxyuridine. J Biol Chem 2002;277:36304 – 11. Epub 2002 Jul 29.

51. Hsueh CT, Kelsen D, Schwartz GK. UCN-01 suppresses thymidylate synthase gene expression and enhances 5-fluorouracil-induced apoptosis in a sequence-dependent manner. Clin Cancer Res 1998;4:2201 – 6.

52. Ju J, Kane SE, Lenz HJ, Danenberg KD, Chu E, Danenberg PV. Desensitization and sensitization of cells to fluoropyrimidines with different antisenses directed against thymidylate synthase messenger RNA. Clin Cancer Res 1998;4:2229 – 36.

53. Lee JH, Park JH, Jung Y, et al. Histone deacetylase inhibitor enhances 5-fluorouracil cytotoxicity by down-regulating thymidylate synthase in human cancer cells. Mol Cancer Ther 2006;5:3085 – 95.

54. Wada Y, Yoshida K, Suzuki T, et al. Synergistic effects of docetaxel and S-1 by modulating the expression of metabolic enzymes of 5-fluorouracil in human gastric cancer cell lines. Int J Cancer 2006;119: 783 – 91.

55. Ferguson PJ, Collins O, Dean NM, et al. Antisense down-regulation of thymidylate synthase to suppress growth and enhance cytotoxicity of 5-FUdR, 5-FU and Tomudex in HeLa cells. Br J Pharmacol 1999;127: 1777 – 86.

56. Aaronson SA. Growth factors and cancer. Science 1991;254: 1146 – 53.

57. Johnston PG, Lenz HJ, Leichman CG, et al. Thymidylate synthase gene and protein expression correlate and are associated with response to 5-fluorouracil in human colorectal and gastric tumors. Cancer Res 1995; 55:1407 – 12.

58. Leichman CG, Lenz HJ, Leichman L, et al. Quantitation of intratumoral thymidylate synthase expression predicts for disseminated colorectal cancer response and resistance to protracted-infusion fluorouracil and weekly leucovorin. J Clin Oncol 1997;15:3223 – 9.

59. Pestalozzi BC, Peterson HF, Gelber RD, et al. Prognostic importance of thymidylate synthase expression in early breast cancer. J Clin Oncol 1997;15:1923 – 31.

60. Johnston PG, Mick R, Recant W, et al. Thymidylate synthase expression and response to neoadjuvant chemotherapy in patients with advanced head and neck cancer. J Natl Cancer Inst 1997;89:308 – 13.

61. Hanada N, Lo HW, Day CP, Pan Y, Nakajima Y, Hung MC. Co-regulation of B-Myb expression by E2F1 and EGF receptor. Mol Carcinog 2006;45:10 – 7.

62. Ginsberg D. EGFR signaling inhibits E2F1-induced apoptosis *in vivo*: implications for cancer therapy. Sci STKE 2007;pe4.

63. Suenaga M, Yamaguchi A, Soda H, et al. Antiproliferative effects of gefitinib are associated with suppression of E2F-1 expression and telomerase activity. Anticancer Res 2006;26:3387 – 91.

64. Nakagawa K, Tamura T, Negoro S, et al. Phase I pharmacokinetic trial of the selective oral epidermal growth factor receptor tyrosine kinase inhibitor gefitinib ("Iressa," ZD1839) in Japanese patients with solid malignant tumors. Ann Oncol 2003;14:922 – 30.

65. Barber TD, Vogelstein B, Kinzler KW, Velculescu VE. Somatic mutations of EGFR in colorectal cancers and glioblastomas. N Engl J Med 2004;351:2883.

66. Lee JW, Soung YH, Kim SY, et al. Absence of EGFR mutation in the kinase domain in common human cancers besides non-small cell lung cancer. Int J Cancer 2005;113:510 – 1.

67. Shigematsu H, Gazdar AF. Somatic mutations of epidermal growth factor receptor signaling pathway in lung cancers. Int J Cancer 2006;118: 257 – 62.

68. Herskovic A, Martz K, al-Sarraf M, et al. Combined chemotherapy and radiotherapy compared with radiotherapy alone in patients with cancer of the esophagus. N Engl J Med 1992;326:1593 – 8.

69. Vanhoefer U, Rougier P, Wilke H, et al. Final results of a randomized phase III trial of sequential high-dose methotrexate, fluorouracil, and doxorubicin versus etoposide, leucovorin, and fluorouracil versus infusional fluorouracil and cisplatin in advanced gastric cancer: a trial of the European Organization for Research and Treatment of Cancer Gastrointestinal Tract Cancer Cooperative Group. J Clin Oncol 2000;18:2648 – 57.

70. Gibson MK, Li Y, Murphy B, et al. Randomized phase III evaluation of cisplatin plus fluorouracil versus cisplatin plus paclitaxel in advanced head and neck cancer (E1395): an Intergroup Trial of the Eastern Cooperative Oncology Group. J Clin Oncol 2005;23:3562 – 7.

Efficacy and Safety of Two Doses of Pemetrexed Supplemented with Folic Acid and Vitamin B_{12} in Previously Treated Patients with Non-Small Cell Lung Cancer

Yuichiro Ohe,[1] Yukito Ichinose,[2] Kazuhiko Nakagawa,[3] Tomohide Tamura,[1] Kaoru Kubota,[4] Nobuyuki Yamamoto,[5] Susumu Adachi,[6] Yoshihiro Nambu,[7] Toshio Fujimoto,[7] Yutaka Nishiwaki,[4] Nagahiro Saijo,[4] and Masahiro Fukuoka[3]

Abstract

Purpose: The objective of this study was to evaluate the efficacy and safety of two doses of pemetrexed supplemented with folic acid and vitamin B_{12} in pretreated Japanese patients with advanced non-small cell lung cancer (NSCLC).

Experimental Design: Patients with an Eastern Cooperative Oncology Group performance status 0 to 2, stage III or IV, and who received previously one or two chemotherapy regimens were randomized to receive 500 mg/m^2 pemetrexed (P500) or 1,000 mg/m^2 pemetrexed (P1000) on day 1 every 3 weeks. The primary endpoint was response rate.

Results: Of the 216 patients evaluable for efficacy (108 in each arm), response rates were 18.5% (90% confidence interval, 12.6-25.8%) and 14.8% (90% confidence interval, 9.5-21.6%), median survival times were 16.0 and 12.6 months, 1-year survival rates were 59.2% and 53.7%, and median progression-free survival were 3.0 and 2.5 months for the P500 and P1000, respectively. Cox multiple regression analysis indicated that pemetrexed dose was not a significant prognostic factor. Drug-related toxicity was generally tolerable for both doses; however, the safety profile of P500 showed generally milder toxicity. Main adverse drug reactions of severity grade 3 or 4 were neutrophil count decreased (20.2%) and alanine aminotransferase (glutamine pyruvic transaminase) increased (15.8%) in P500 and neutrophil count decreased (24.3%), WBC count decreased (20.7%), and lymphocyte count decreased (18.0%) in P1000. One drug-related death from interstitial lung disease occurred in the P500.

Conclusion: P500 and P1000 are similarly active with promising efficacy and acceptable safety outcomes in pretreated patients with NSCLC. These results support the use of P500 as a second- and third-line treatment of NSCLC.

Pemetrexed (LY231514; Alimta), a multitargeted antifolate, has shown antitumor activity as a single agent or in combination with other anticancer agents (1, 2). Pemetrexed at doses of 500 or 600 mg/m^2 has been evaluated in various clinical settings in a broad range of tumors including lung (non-small cell and mesothelioma), colorectal, gastric, pancreatic, head and neck, bladder, cervical, and breast cancers (3–13). In a randomized phase III trial that compared 3-week regimens of single-agent 500 mg/m^2 pemetrexed versus 75 mg/m^2 docetaxel in pretreated patients with non-small cell lung cancer (NSCLC), respective response rates (9.1% versus 8.8%) and median survival times (MST; 8.3 versus 7.9 months) did not differ between pemetrexed and docetaxel. However, fewer hematologic adverse effects, such as grade 3 or 4 neutropenia, febrile neutropenia, and neutropenic fever, were observed in patients treated with pemetrexed (3).

Myelosuppression is the predominant dose-limiting toxicity of pemetrexed as reported in phase I studies (14–16). A multivariate analysis identified the correlation between poor folate status (as indicated by elevated plasma homocysteine levels) and increased toxicity to pemetrexed, which led to the requirement that patients in all pemetrexed studies receive folic acid and vitamin B_{12} supplementation (2, 17). This has been shown to decrease toxicity to pemetrexed without compromising efficacy (18). Without supplementation, the maximum tolerated dose of pemetrexed, given every 3 weeks, has been shown to be 600 mg/m^2 in heavily pretreated patients (14); however, with supplementation, higher pemetrexed doses have been given without limiting side effects. In a Japanese phase I

Authors' Affiliations: [1]Department of Internal Medicine, National Cancer Center Hospital, Tokyo, Japan; [2]National Kyushu Cancer Center, Fukuoka, Japan; [3]Kinki University School of Medicine, Osakasayama, Japan; [4]National Cancer Center Hospital East, Kashiwa, Japan; [5]Shizuoka Cancer Center Hospital, Shizuoka, Japan; [6]Eli Lilly and Company, Oncology Platform Team, Indianapolis, Indiana; and [7]Eli Lilly Japan K.K., Lilly Research Laboratories Japan, Kobe, Japan

Received 12/11/07; revised 3/6/08; accepted 3/19/08.

Grant support: Eli Lilly and Company (study code: H3E-JE-NS01).

The costs of publication of this article were defrayed in part by the payment of page charges. This article must therefore be hereby marked *advertisement* in accordance with 18 U.S.C. Section 1734 solely to indicate this fact.

Note: The results of this study have been reported at American Society of Clinical Oncology, World Conference on Lung Cancer, and European Cancer Conference in 2007.

Requests for reprints: Yuichiro Ohe, Department of Internal Medicine, National Cancer Center Hospital, 5-1-1 Tsukiji, Chuo-ku, Tokyo 104-0045, Japan. Phone: 81-3-3542-2511; Fax: 81-3-3542-7006; E-mail: yohe@ncc.go.jp.

doi:10.1158/1078-0432.CCR-07-5143

study of pemetrexed that included folic acid and vitamin B_{12} supplementation, the maximum tolerated dose of pemetrexed was 1,200 mg/m^2 and recommended dose was 1,000 mg/m^2 given every 3 weeks (19). Pemetrexed pharmacokinetics in Japanese patients was not overtly different from those observed in Caucasian patients.

In view of these data, we conducted a randomized, phase II study that confirmed the efficacy and safety of a standard dose of pemetrexed (500 mg/m^2; P500) with that of a higher dose (1,000 mg/m^2; P1000), including folic acid and vitamin B_{12} supplementation, in previously treated NSCLC patients. The primary endpoint was evaluation of response rate. Secondary endpoints were assessments of response duration, progression-free survival (PFS), 1-year survival rate, MST, quality of life (QoL), and adverse events.

Materials and Methods

Patient selection. Men and women, between 20 and 75 years old, with a life expectancy of at least 12 weeks and histologically and/or cytologically confirmed advanced NSCLC were eligible for the study. In addition, all patients met the following inclusion criteria: stage III or IV disease, at least one target lesion, one or two prior chemotherapeutic regimens, an Eastern Cooperative Oncology Group performance status (PS) of 0 to 2, adequate bone marrow function (neutrophils ≥2,000/mm^3, platelets ≥100,000/mm^3, and hemoglobin ≥9.0 g/dL), hepatic function [total bilirubin within 1.5 times the upper normal limit, aspartate aminotransferase (AST) and alanine aminotransferase (ALT) within 2.5 times the upper normal limit, and serum albumin ≥2.5 g/dL], renal function (serum creatinine ≤1.2 mg/dL and creatinine clearance ≥45 mL/min), and pulmonary function (functional oxygen saturation ≥92%).

Patients were excluded from the study for radiographic signs of interstitial pneumonitis or pulmonary fibrosis, serious or uncontrolled concomitant systemic disorders, active infections, the need for chronic administration of systemic corticosteroids, active double cancer and/or brain metastases, treatment with third-space fluid collections within 2 weeks of signing the informed consent or the need of such treatment, grade 3 or 4 toxicity, peripheral sensory neuropathy, previous pemetrexed therapy, unable or unwilling to take folic acid or vitamin B_{12} supplementation, or pregnant or breast-feeding.

This study was conducted in compliance with the guidelines of good clinical practice and the principles of the Declaration of Helsinki, and it was approved by the local institutional review boards. All patients gave written informed consent before study entry.

Study design and sample size. This open-label multicenter study had response rate as the primary objective, and 244 patients were enrolled and 226 were allocated to either 500 mg/m^2 (P500) or 1,000 mg/m^2 (P1000) randomly.

The sample size was calculated to ensure that the response rate in each group exceeded 5%. Based on the results from previous study, assuming a 13% true response rate, 5% one-sided significance level for the test with exact probability based on binomial distribution, and 90% power, at least 107 patients in each treatment arm (total of 214) were necessary. Assuming a 10% dropout rate, 240 patients were planned for the study (actual: 244 patients).

The randomization was done by an independent registration center and was dynamically balanced for PS, previous platinum chemotherapy, disease stage, gender, time from prior chemotherapy to the enrollment, and hospital. Patients were balanced with respect to the study drug in each stratum for each prognostic factor using the minimization method.

Treatment plan. Pemetrexed was administered as an i.v., 10-min infusion on day 1 of a 21-day cycle. Patients were instructed to take orally 1 g/d of a multivitamin containing 500 μg folic acid from 1 week before day 1 of course 1 until 22 days after the last administration of pemetrexed. Vitamin B_{12} (1000 μg) was injected i.m. 1 week before day 1 of course 1 and repeated every 9 weeks until 22 days after the last administration of pemetrexed. Patients were discontinued from the study for disease progression, unacceptable adverse events, inadvertent enrollment, use of excluded concomitant therapy, a cycle delay of >42 days, or if the patient requested to discontinue the study.

Administration of pemetrexed was delayed if patients met any of the following criteria: neutrophils <2,000/mm^3, hemoglobin <9.0 g/dL, platelets <100,000/mm^3, AST/ALT >2.5 times the upper normal limit, total bilirubin >1.5 times the upper normal limit, serum creatinine >1.2 mg/dL, PS 3 or 4, or grade ≥3 nonhematologic toxicity (except for anorexia, nausea, vomiting, and fatigue). The dose of pemetrexed was decreased to 400 mg/m^2 in the P500 arm and to 800 mg/m^2 in the P1000 arm, if any of the following events occurred in the previous course: grade 4 leukopenia or neutropenia, grade ≥3 febrile neutropenia, thrombocytopenia, or platelet transfusion, grade ≥3 nonhematologic toxicity (except for grade 3 anorexia, nausea, vomiting, and fatigue), or AST/ALT increased. The pemetrexed dose was similarly reduced if initiation of the next course was postponed after day 29 due to drug-related adverse events. Patients who continued to show evidence of toxicity after reducing the pemetrexed dose were discontinued from the study.

Baseline and treatment assessments. Pretreatment assessments included chest X-ray, electrocardiogram, blood chemistry, urinalysis, pregnancy test, creatinine clearance, functional oxygen saturation, vital signs, PS, body weight, and use of prior therapies. Tumor size was examined using X-ray, computer tomography, or magnetic resonance imaging done within 28 days before the planned day of the first treatment. This was repeated about every 4 weeks after the first examination.

Tumor response rate was assessed as the percentage of patients in whom complete response (CR) and partial response (PR) were confirmed based on the best overall response of the tumor response evaluation. Response was evaluated according to the Response Evaluation Criteria in Solid Tumors (20). Objective tumor responses in all responding patients were evaluated by an external review committee given no information on the treatment groups.

Duration of overall response (CR + PR) was measured from the date of the first objective assessment of CR or PR until the date of progressive disease. PFS was measured from the date of registration (for the initiation of course 1) until the date of progressive disease or death. One-year survival rate was defined as the percentage of patients who survived for 1 year from the registration date. Survival was measured from the registration date to the date of death (regardless of cause).

QoL was assessed by the QoL Questionnaire for Cancer Patients Treated with Anticancer Drugs and the Functional Assessment of Cancer Therapy for Lung Cancer (Japanese version; refs. 21–23).

Assessments of QoL were done before treatment, before the second and third courses of chemotherapy, and 3 months after the start of treatment.

Adverse events were recorded throughout the study and after the last drug administration until signs of recovery were evident. All such events were evaluated according to the Common Terminology Criteria for Adverse Events version 3.0.

Statistical analysis. Efficacy measurements were done according to the guidelines for clinical evaluation methods of anticancer drugs. Efficacy analysis was done on patients who met all selection criteria and received at least one dose of pemetrexed. Safety analysis was done on patients who received at least one dose of pemetrexed.

Statistical tests were done to establish a pemetrexed response rate of >5%; 90% confidence intervals (CI) for the objective response rate were constructed for each arm. All survival curves for time-to-event variables were created using the Kaplan-Meier method; 95% CIs were calculated for each arm. Response rate, response duration, and PFS were compared between the two arms using the χ^2 test. Cox multiple regression analysis was done on all evaluable patients from two combined arms to

identify significant prognostic factors for survival. Covariates evaluated were pemetrexed dose, gender, age, PS, disease stage, histology, interval from prior chemotherapy to registration for the first treatment course, the number of prior chemotherapeutic regimens, and use of prior platinum chemotherapy. For the QoL analysis, distributions of subscales were summarized for each arm using descriptive statistics (mean, SD, minimum, median, and maximum). As a retrospective analysis for safety, major grade 3 to 4 drug-related adverse events were compared between the two arms using the χ^2 test.

Results

Patient disposition and characteristics. From October 2004 to October 2005, a total of 244 Japanese patients with advanced NSCLC were enrolled at 28 centers. Of the 244 patients enrolled, 226 were randomly assigned (114 to the P500 arm and 112 to the P1000 arm) at least 1 week before treatment after receiving folic acid and vitamin B_{12} supplementation. A total of 225 patients (114 in the P500 arm and 111 in P1000 arm) were evaluable for safety. Of these patients, 216 (108 in each arm) were evaluable for efficacy. Gender, age, PS, histology, stage, and prior platinum chemotherapy were well balanced across the two arms (Table 1).

Efficacy evaluation. Objective tumor response rates and durations of overall response are shown in Table 2. Of the 108 patients evaluable for efficacy in the P500 arm, 20 achieved PR for an objective response rate of 18.5% (90% CI, 12.6-25.8%); the median duration of response was 4.9 months (95% CI, 3.8-8.7 months). Of the 108 patients evaluable for efficacy in the P1000 arm, 16 achieved PR for an objective response rate of 14.8% (90% CI, 9.5-21.6%); the median duration of response was 3.0 months (95% CI, 2.8-6.1 months). As seen above, the lower limits of the 90% CI in both arms were >5%, showing a statistically significant objective response rate >5% in each of the arms. The differences between arms in response rate and response duration were not statistically significant (P = 0.5839 and 0.1740).

By October 2006, 125 of the 216 evaluable patients had died. The MST and 1-year survival rate were 16.0 months and 59.2% in the P500 arm and 12.6 months and 53.7% in the P1000 arm (P = 0.1463, log-rank test for survival; Fig. 1). Median PFS was 3.0 months (95% CI, 2.0-3.5 months) in the P500 arm and 2.5 months (95% CI, 1.8-3.2 months) in the P1000 arm (P = 0.7139, log-rank test).

Cox multiple regression analysis indicated that pemetrexed dose was not a significant prognostic factor; however, gender (female), PS (0), disease stage (III), histologic type (non-squamous cell carcinoma), and longer intervals from prior chemotherapy were shown to be good prognostic factors (Fig. 2). Of note, patients with non-squamous cell carcinoma had a longer MST compared with those with other histologic types (16.0 versus 9.3 months; P = 0.00264, Cox regression analysis). Pretreatment QoL assessments in both arms were relatively high and showed neither worsening nor improvement following pemetrexed treatment (Table 3).

Safety evaluation. A total of 225 patients (114 for P500 and 111 for P1000) were evaluable for safety. Leukopenia, neutropenia, lymphopenia, anemia, elevation of AST/ALT, lactate dehydrogenase, and rash were commonly reported; however, no grade 4 leukopenia or febrile neutropenia was observed (Table 4). Other grade 4 toxicities were uncommon. Gastrointestinal toxicities such as nausea, vomiting, and anorexia were mostly mild and more frequently reported in the P1000 arm. As a retrospective analysis for safety, major grade 3 to 4 drug-related adverse events were compared

Table 1. Patient characteristics

Variable	P500	P1000
Patients who were given at least one dose of pemetrexed	114	111
Gender		
Male	72	71
Female	42	40
Age, median (range)	61.0 (37-74)	62.0 (26-74)
Eastern Cooperative Oncology Group PS		
0	45	37
1	63	68
2	6	6
Histology		
Adenocarcinoma	79	82
Squamous cell carcinoma	25	26
Others	10	3
Disease stage		
III	22	22
IV	92	88
No. prior chemotherapies		
1	44	53
2	67	57
3	3	1
Prior platinum chemotherapy		
Yes	108	104
No	6	7
Interval from prior chemotherapy to registration for the first course starts (mo)		
<3	72	66
3	42	45

Table 2. Objective tumor response and median response duration

Variable	P500 (n = 108)	P1000 (n = 108)
Objective tumor response		
CR	0	0
PR	20	16
Stable disease	40	34
Progressive disease	48	58
Response rate (90% CI), %	18.50 (12.6-25.8)	14.80 (9.5-21.6)
Median response duration (95% CI), mo	4.9 (3.8-8.7)	3.0 (2.8-6.1)

between the two arms using the χ^2 test. Grade 3 or 4 anorexia was reported more frequently in the P1000 arm (10.8% versus 2.6%; P = 0.0284). Drug-related rash was observed in 67.5% and 80.2% of the patients treated with P500 and P1000, respectively. However, all severities were grade 1 or 2. Five of the P500 patients and 3 of the P1000 patients developed interstitial lung disease related to pemetrexed treatment that resulted in the death of one patient (P500 arm). The other 7 patients recovered from their illness after discontinuing the study drug. A total 16 (14.0%) patients in the P500 arm and 26 (23.4%) patients in the P1000 arm discontinued the treatment because of drug-related adverse events.

Dose administration. The median number of treatment courses completed in both arms was 3 (range, 1-24+). Eleven percent of patients in the P500 arm and 8% in the P1000 arm completed at least 10 courses. Dose reduction occurred in 20 (17.5%) patients in the P500 arm and 27 (24.3%) patients in the P1000 arm. The most frequent cause of dose reduction was ALT elevation. Relative dose intensities were 89.6% in the P500 group and 89.8% in the P1000 group.

Discussion

This phase II, randomized study is the first report on the efficacy and safety of a higher dose of pemetrexed (1,000 mg/m^2) in pretreated Japanese patients with NSCLC. Most patients (>50%) received two courses of prior chemotherapy, and the vast majority or patients (>90%) received prior platinum-based chemotherapy. The response data indicate promising tumor reduction activity and are noteworthy in pretreated patients. The survival data are also promising and better than those reported in second- and third-line settings and comparable with those reported in first-line settings (3, 24, 25). In the phase III study (3) comparing pemetrexed with docetaxel, the response

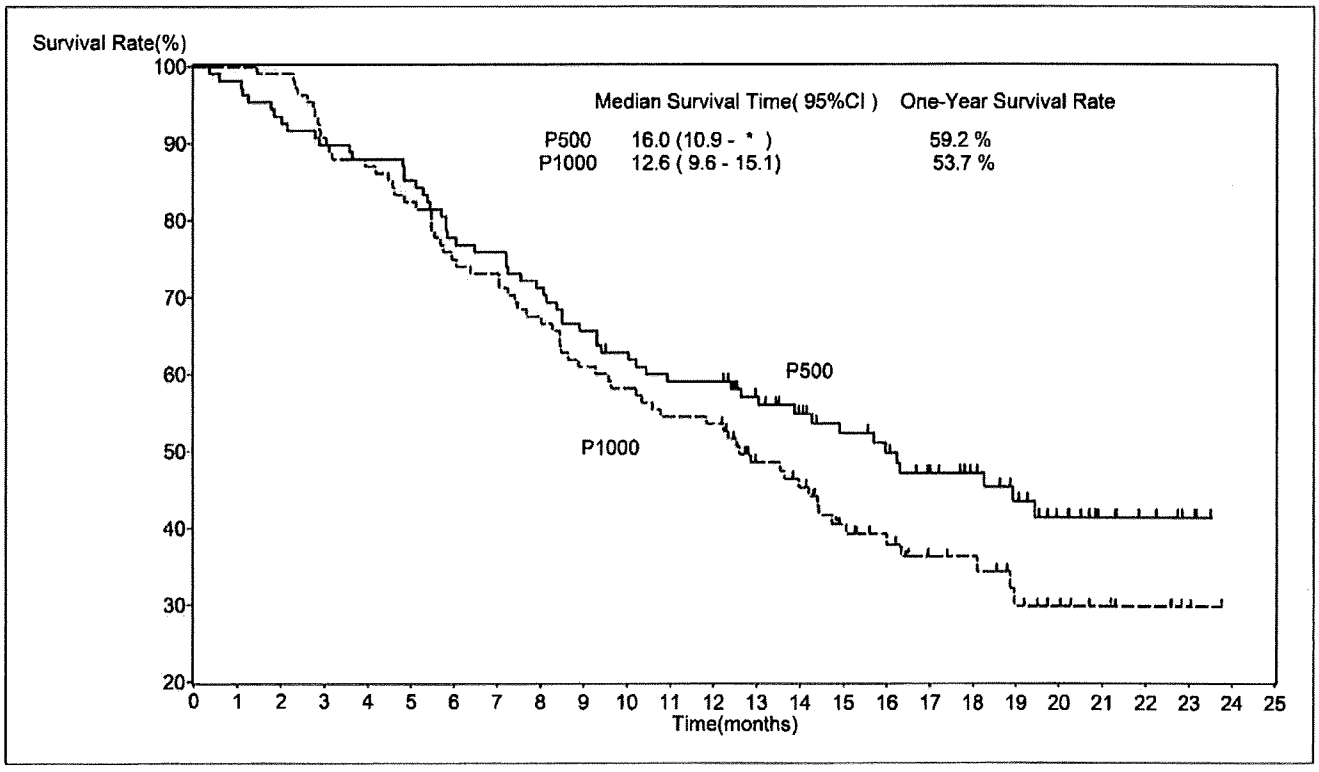

Fig. 1. Kaplan-Meier curve showing the overall survival for each arm. *Asterisk*, upper limit could not be calculated because of the censoring at the end of study period.

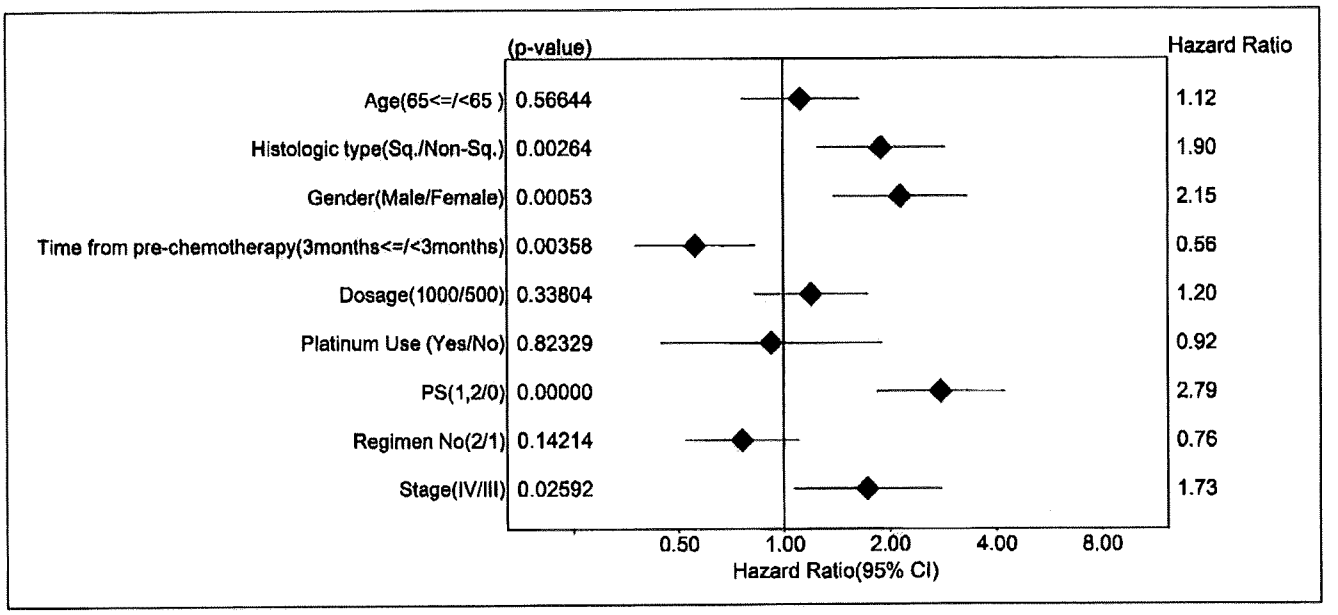

Fig. 2. Forest plot. Cox multiple regression analysis was done on all evaluable patients from two combined arms to identify significant prognostic factors for survival. Covariates evaluated were pemetrexed dose, gender, age, PS, disease stage, histology, interval from prior chemotherapy to registration for the first treatment course, the number of prior chemotherapeutic regimens, and use of prior platinum chemotherapy.

rate and median survival in the pemetrexed arm were 9.1% and 8.3 months, respectively.

Both P500 and P1000 with folic acid and vitamin B_{12} supplementation were similarly active in previously treated patients with NSCLC. All efficacy measures were similar in both arms as shown by the response rate, survival, and PFS, suggesting that doubling the standard dose of pemetrexed does not show superior efficacy. In addition, Cox multiple regression analysis showed that the difference of pemetrexed dose did not influence survival. Overall, toxicity was more frequent at the higher dose, although toxicity in both arms was mild.

Cullen et al. reported a randomized trial of 500 versus 900 mg/m^2 pemetrexed in patients with advanced NSCLC treated previously with platinum-based chemotherapy (26). The response rate, median PFS, and median survival were 7.1%, 2.6 months, and 6.7 months in patients treated with 500 mg/m^2 and 4.3%, 2.8 months, and 6.9 months in patients treated with 900 mg/m^2 pemetrexed, respectively. The higher dose did not improve survival more than the lower dose.

Dose intensification is not always accompanied by higher efficacy, such as in the case of docetaxel and cisplatin. One possible explanation for this in pemetrexed is that either the intracellular transport of pemetrexed is maximal at 500 mg/m^2 or the inhibition of target enzymes is saturated above this dose; however, there are as yet no *in vitro* data to support either mechanism. Although the mechanism still needs to be elucidated, the wide therapeutic window of pemetrexed makes it unique and safe for patients.

Of interest, our subgroup analysis identified some prognostic factors. The subgroups that were identified as good prognostic factors, gender (female), good PS, early-stage disease, and longer intervals from prior chemotherapy are well known as good prognostic factors for NSCLC. Of particular note, the MST

Table 3. Summary for Functional Assessment of Cancer Therapy for Lung Cancer Lung Cancer Subscale

	n	Mean (SD)	Min	Med	Max
P500 (*n* = 108)					
Before course 1	107	71.5 (18.81)	32.1	71.4	100
Before course 2	101	74.3 (16.68)	39.3	75	100
Before course 3	84	74.3 (18.08)	35.7	78.6	100
Registration of course 1 + 3 mo*	59	76.3 (18.1)	32.1	78.6	100
P1000 (*n* = 108)					
Before course 1	107	69.6 (18.52)	25	67.9	100
Before course 2	98	73.5 (17.21)	32.1	75	100
Before course 3	72	71.4 (18.4)	28.6	71.4	100
Registration of course 1 + 3 mo*	61	74.3 (18.62)	28.6	71.4	100

*Three months ±2 weeks after the day of registration for one course.

Table 4. Hematologic and nonhematologic toxicity evaluated by Common Terminology Criteria for Adverse Events version 3.0

	P500 (n = 114)				P1000 (n = 111)				P
	Grade (%)				Grade (%)				
	2	3	4	3/4/5	2	3	4	3/4/5	
Leukopenia	32.5	14.9	0	14.9	38.7	21.6	0	21.6	0.2582
Neutropenia	25.4	17.5	3.5	21.1	27.9	19.8	4.5	24.3	0.6695
Lymphopenia	28.9	9.6	2.6	12.3	30.6	16.2	1.8	18	0.31
Anemia	19.3	7	0.9	7.9	34.2	9	0.9	9.9	0.7667
Thrombocytopenia	0	0	0	0	8.1	0.9	0	0.9	NA
Febrile neutropenia	*	0	0	0	*	0	0	0	NA
Nausea	14	0	0	0	14.4	2.7	0	2.7	NA
Vomiting	7	0	0	0	11.7	1.8	0	1.8	NA
Anorexia	16.7	2.6	0	2.6	15.3	10.8	0	10.8	0.0284
Fatigue	3.5	0	0	0	1.8	0.9	0	0.9	NA
Diarrhea	2.6	0.9	0	0.9	1.8	1.8	0	1.8	0.9815
Constipation	1.8	0.9	0	0.9	5.4	0	0	0	NA
Rash	49.1	2.6	0	2.6	63.1	4.5	0	4.5	0.6903
Alopecia	0	*	*	*	0	*	*	*	NA
Pneumonitis	1.8	1.8	0	2.6†	0	2.7	0	2.7	1
AST	21.9	7.9	0	7.9	25.2	4.5	0	4.5	0.4375
ALT	17.5	16.7	0	16.7	32.4	7.2	0.9	8.1	0.8143

NOTE: Major grade 3 to 4 drug-related adverse events were compared between two arms using χ^2 test.
*Not indicated in Common Terminology Criteria for Adverse Events version 3.0.
† One patient died of drug-induced pneumonitis.

of patients with non-squamous cell carcinoma was significantly longer compared with that in patients with squamous cell carcinoma (16.0 versus 9.3 months; P = 0.00264). Pemetrexed induces its antitumor activity by inhibiting key enzymes related to the folate metabolism, such as thymidylate synthase. Studies of the tumor histology of adenocarcinoma progressive disease have reported lower-level expression of thymidylate synthase than squamous cell carcinoma (27). Good survival benefit in patients with non-squamous cell carcinoma by pemetrexed may be explained by lower levels of thymidylate synthase. Because MST was the subject of a subgroup analysis and survival was not a primary endpoint of this study, this finding should be considered exploratory requiring independent confirmation. However, if this finding of superior effectiveness in non-squamous cell carcinoma could be substantiated in future studies, it would be very useful. Indeed, histology could be a simple means of tailoring chemotherapy treatment.

In conclusion, although the recommended dose is P1000 with folic acid and vitamin B_{12} supplementation for Japanese patients, it has similar efficacy and safety with P500, the recommend dosage in rest of the world. These results support the use of P500 as a second- or third-line treatment of NSCLC.

Disclosure of Potential Conflicts of Interest

Authors have conflicts with Eli Lilly and company.

Acknowledgments

We thank the physicians who enrolled patients (Drs. Hiroshi Isobe, Akira Inoue, Yoshio Tomizawa, Akira Yokoyama, Shuichi Yoneda, Masaru Narabayashi, Masahiko Shibuya, Masahiro Tsuboi, Hiroaki Okamoto, Kenji Eguchi, Toshiyuki Sawa, Koji Takeda, Fumio Imamura, Shinzoh Kudoh, Masaaki Kawahara, Kaoru Matsui, Nobuyuki Katakami, Shunichi Negoro, Katsuyuki Kiura, Yoshihiko Segawa, Koichi Takayama, Mitsuhiro Matsumoto, and Takeshi Horai) and Michiyo Matsushima for assistance in the creation and submission of this article.

References

1. Walling J. From methotrexate to pemetrexed and beyond. A review of the pharmacodynamic and clinical properties of antifolates. Invest New Drugs 2006;24:37–77.
2. Hazarika M, White RM, Johnson JR, Pazdur R. FDA drug approval summaries: pemetrexed (Alimta®). Oncologist 2004;9:482–8.
3. Hanna N, Shepherd FA, Fossella FV, et al. Randomized phase III trial of pemetrexed versus docetaxel in patients with non-small-cell lung cancer previously treated with chemotherapy. J Clin Oncol 2004;22:1589–97.
4. Vogelzang NJ, Rusthoven JJ, Symanowski J, et al. Phase III study of pemetrexed in combination with cisplatin versus cisplatin alone in patients with malignant pleural mesothelioma. J Clin Oncol 2003;21:2636–44.
5. John W, Picus J, Blanke CD, et al. Activity of multitargeted antifolate (pemetrexed disodium, LY231514) in patients with advanced colorectal carcinoma: results from a phase II study. Cancer 2000;88:1807–13.
6. Cripps C, Burnell M, Jolivet J, et al. Phase II study of first-line LY231514 (multi-targeted antifolate) in patients with locally advanced or metastatic colorectal cancer: an NCIC Clinical Trials Group study. Ann Oncol 1999;10:1175–9.
7. Bajetta E, Celio L, Buzzoni R, et al. Phase II study of pemetrexed disodium (Alimta®) administered with oral folic acid in patients with advanced gastric cancer. Ann Oncol 2003;14:1543–8.
8. Miller KD, Picus J, Blanke C, et al. Phase II study of the multitargeted antifolate LY231514 (Alimta, MTA, pemetrexed disodium) in patients with advanced pancreatic cancer. Ann Oncol 2000;11:101–3.
9. Pivot X, Raymond E, Laguerre B, et al. Pemetrexed disodium in recurrent locally advanced or metastatic squamous cell carcinoma of the head and neck. Br J Cancer 2001;85:649–55.
10. Hanauske AR, Chen V, Paoletti P, Niyikiza C. Pemetrexed disodium: a novel antifolate clinically active against multiple solid tumors. Oncologist 2001;6:363–73.
11. Goedhals L, van Wiyk AL, Smith BL, Fourie SJ. Pemetrexed (Alimta, LY231514) demonstrates clinical activity in chemonaive patients with cervical cancer in a phase II single-agent trial. Int J Gynecol Cancer 2006;16:1172–8.
12. Miles DW, Smith IE, Coleman RE, Calvert AH, Lind MJ. A phase II study of pemetrexed disodium (LY231514) in patients with locally recurrent or metastatic breast cancer. Eur J Cancer 2001;37:1366–71.

13. Martin M, Spielmann M, Namer M, et al. Phase II study of pemetrexed in breast cancer patients pretreated with anthracyclines. Ann Oncol 2003;14:1246–52.
14. Rinaldi DA, Kuhn JG, Burris HA, et al. A phase I evaluation of multitargeted antifolate (MTA, LY231514), administered every 21 days, utilizing the modified continual reassessment method for dose escalation. Cancer Chemother Pharmacol 1999;44:372–80.
15. Rinaldi DA, Burris HA, Dorr FA, et al. Initial phase I evaluation of the novel thymidylate synthase inhibitor, LY231514, using the modified continual reassessment method for dose escalation. J Clin Oncol 1995;13:2842–50.
16. McDonald AC, Vasey PA, Adams L, et al. A phase I and pharmacokinetic study of LY231514, the multitargeted antifolate. Clin Cancer Res 1998;4:605–10.
17. Niyikiza C, Baker SD, Seitz DE, et al. Homocysteine and methylmalonic acid: markers to predict and avoid toxicity from pemetrexed therapy. Mol Cancer Ther 2002;1:545–52.
18. Scagliotti GV, Shin DM, Kindler HL, et al. Phase II study of pemetrexed with and without folic acid and vitamin B_{12} as front-line therapy in malignant pleural mesothelioma. J Clin Oncol 2003;21:1556–61.
19. Nakagawa K, Kudoh S, Matsui K, et al. A phase I study of pemetrexed (LY231514) supplemented with folate and vitamin B_{12} in Japanese patients with solid tumours. Br J Cancer 2006;95:677–82.
20. Therasse P, Arbuck SG, Eisenhauer EA, et al. New guidelines to evaluate the response to treatment in solid tumors. J Natl Cancer Inst 2000;92:205–16.
21. Cella DF, Bonomi AE, Lloyd SR, Tulsky DS, Kaplan E, Bonomi P. Reliability and validity of the Functional Assessment of Cancer Therapy-Lung (FACT-L) quality of life instrument. Lung Cancer 1995;12:199–220.
22. Kurihara M, Shimizu H, Tsuboi K, et al. Development of quality of life questionnaire in Japan: quality of life assessment of cancer patients receiving chemotherapy. Psychooncology 1999;8:355–63.
23. Matsumoto T, Ohashi Y, Morita S, et al. The quality of life questionnaire for cancer patients treated with anticancer drugs (QOL-ACD): validity and reliability in Japanese patients with advanced non-small-cell lung cancer. Qual Life Res 2002;11:483–93.
24. Shepherd FA, Dancey J, Ramlau R, et al. Prospective randomized trial of docetaxel versus best supportive care in patients with non-small-cell lung cancer previously treated with platinum-based chemotherapy. J Clin Oncol 2000;18:2095–103.
25. Ohe Y, Ohashi Y, Kubota K, et al. Randomized phase III study of cisplatin plus irinotecan versus carboplatin plus paclitaxel, cisplatin plus gemcitabine, and cisplatin plus vinorelbine for advanced non-small-cell lung cancer: Four-Arm Cooperative Study in Japan. Ann Oncol 2007;18:317–23.
26. Cullen M, Zatloukal P, Sörenson S, et al. Pemetrexed for the treatment of advanced non-small cell lung cancer (NSCLC): results from a randomized phase III dose finding trial in patients who progressed following platinum-containing chemotherapy. J Thorac Oncol 2007;2:S316–7.
27. Ceppi P, Volante M, Saviozzi S, et al. Squamous cell carcinoma of the lung compared with other histotypes shows higher messenger RNA and protein levels for thymidylate synthase. Cancer 2006;107:1589–96.

Radiosensitizing Effect of YM155, a Novel Small-Molecule Survivin Suppressant, in Non–Small Cell Lung Cancer Cell Lines

Tsutomu Iwasa,[1] Isamu Okamoto,[1] Minoru Suzuki,[2] Takahito Nakahara,[4] Kentaro Yamanaka,[4] Erina Hatashita,[1] Yuki Yamada,[1] Masahiro Fukuoka,[3] Koji Ono,[2] and Kazuhiko Nakagawa[1]

Abstract

Purpose: Survivin, a member of the inhibitor of apoptosis protein family, is an attractive target for cancer therapy. We have now investigated the effect of YM155, a small-molecule inhibitor of survivin expression, on the sensitivity of human non–small cell lung cancer (NSCLC) cell lines to γ-radiation.

Experimental Design: The radiosensitizing effect of YM155 was evaluated on the basis of cell death, clonogenic survival, and progression of tumor xenografts. Radiation-induced DNA damage was evaluated on the basis of histone H2AX phosphorylation and foci formation.

Results: YM155 induced down-regulation of survivin expression in NSCLC cells in a concentration- and time-dependent manner. A clonogenic survival assay revealed that YM155 increased the sensitivity of NSCLC cells to γ-radiation *in vitro*. The combination of YM155 and γ-radiation induced synergistic increases both in the number of apoptotic cells and in the activity of caspase-3. Immunofluorescence analysis of histone γ-H2AX also showed that YM155 delayed the repair of radiation-induced double-strand breaks in nuclear DNA. Finally, combination therapy with YM155 and γ-radiation delayed the growth of NSCLC tumor xenografts in nude mice to a greater extent than did either treatment modality alone.

Conclusions: These results suggest that YM155 sensitizes NSCLC cells to radiation both *in vitro* and *in vivo*, and that this effect of YM155 is likely attributable, at least in part, to the inhibition of DNA repair and enhancement of apoptosis that result from the down-regulation of survivin expression. Combined treatment with YM155 and radiation warrants investigation in clinical trials as a potential anticancer strategy.

Survivin is a 16.5-kDa member of the inhibitor of apoptosis protein (IAP) family. It blocks the mitochondrial pathway of apoptosis by inhibiting caspases (1, 2) and regulates cell division through interaction with the proteins INCENP and Aurora B (3). It is abundant in many types of cancer cells but not in the corresponding normal cells (4–6). High levels of survivin expression in cancer cells are associated with poor patient prognosis and survival as well as with resistance to therapy and an increased rate of cancer recurrence (7–9). Survivin has therefore become a therapeutic target and potentially important prognostic marker for many tumor types, including non–small cell lung cancer (NSCLC; refs. 7, 10). Molecular antagonists of survivin including antisense oligonucleotides, and dominant negative mutants have been shown to induce apoptosis in cancer cells *in vitro* and *in vivo* as well as to enhance chemotherapy-induced cell death (11–13). Although antisense oligonucleotides and ribozymes can be engineered to be highly specific for survivin, they may be difficult to deliver in the clinical setting.

YM155, a small imidazolium-based compound, was identified by high-throughput screening of chemical libraries for inhibitors of the activity of the survivin gene promoter in a reporter assay (14). This compound specifically inhibits the expression of survivin at both the mRNA and protein levels and exhibits pronounced anticancer activity in preclinical models (14). An advantage of YM155 compared with previously investigated suppressors of survivin expression (15–20) is that it is active in the subnanomolar range. Pharmacokinetic analysis also revealed that YM155 was highly distributed to tumor tissue in tumor xenograft models *in vivo* (14). YM155 is thus an attractive candidate drug for cancer therapy, and clinical trials of YM155 in single-agent therapy are currently under way for some types of cancer.

Glioblastoma cells that overexpress survivin were found to be less responsive to radiation than survivin-negative cells in a preclinical model (21). Clinically, high levels of survivin expression have been associated with an increased risk of local treatment failure after radiochemotherapy in patients with rectal cancer (9). These observations suggest that survivin plays

Authors' Affiliations: [1]Department of Medical Oncology, Kinki University School of Medicine, Osaka-Sayama, Osaka, Japan; [2]Radiation Oncology Research Laboratory, Research Reactor Institute, Kyoto University, Sennan-gun, Osaka, Japan; and [3]Kinki University School of Medicine, Sakai Hospital, Minami-ku Sakai, Osaka, Japan; and [4]Institute for Drug Research, Astellas Pharma, Inc., Tsukuba-shi, Ibaraki, Japan

Received 2/20/08; revised 5/21/08; accepted 6/1/08.

The costs of publication of this article were defrayed in part by the payment of page charges. This article must therefore be hereby marked *advertisement* in accordance with 18 U.S.C. Section 1734 solely to indicate this fact.

Requests for reprints: Isamu Okamoto, Department of Medical Oncology, Kinki University School of Medicine, 377-2 Ohno-higashi, Osaka-Sayama, Osaka 589-8511, Japan. Phone: 81-72-366-0221; Fax: 81-72-360-5000; E-mail: chi-okamoto@dotd.med.kindai.ac.jp.

doi:10.1158/1078-0432.CCR-08-0468

Translational Relevance

Survivin is a potentially important molecular target for cancer therapy. Reflecting the many mechanisms that seem to regulate survivin expression, diverse approaches have been evaluated for targeting survivin in experimental models. YM155 is a novel small, imidazolium-based compound that specifically inhibits survivin expression in various types of cancer cell lines *in vitro*. In addition, YM155 has been shown to distribute preferentially to tumor tissues rather than to plasma as well as to exert pronounced antitumor activity in tumor xenograft models *in vivo*. The use of YM155 as a single agent in phase I clinical trials did not reveal significant toxicity. Although phase II studies of YM155 use as a single agent for certain types of cancer are currently under way, the effects of YM155 in combination with radiation have not been reported. We now show that inhibition of survivin expression by YM155 sensitizes tumor cells to radiation *in vitro* and *in vivo*. Therefore, our preclinical results provide a rationale for future clinical investigation of the therapeutic efficacy of YM155 in combination with radiotherapy.

a role in resistance to radiotherapy. Indeed, suppression of survivin expression with the use of antisense oligonucleotides or ribozymes has been shown to increase the radiosensitivity of cancer cells *in vitro* (20, 22–26). We have now examined the effects of the combination of YM155 and radiation on NSCLC cell lines *in vitro* and *in vivo*.

Materials and Methods

Cell culture and reagents. The human NSCLC cell lines NCI-H460 (H460) and Calu6 were obtained from the American Type Culture Collection. The cells were cultured under an atmosphere of 5% CO_2 at 37°C in RPMI 1640 (Sigma) supplemented with 10% fetal bovine serum. YM155 (Astellas Pharma, Inc.) was dissolved in DMSO.

Immunoblot analysis. Cells were washed twice with ice-cold PBS and then lysed in a solution containing 20 mmol/L Tris-HCl (pH 7.5), 150 mmol/L NaCl, 1 mmol/L EDTA, 1% Triton X-100, 2.5 mmol/L sodium PPi, 1 mmol/L phenylmethylsulfonyl fluoride, and leupeptin (1 μg/mL). The protein concentration of lysates was determined with the Bradford reagent (Bio-Rad), and equal amounts of protein were subjected to SDS-PAGE of a 15% gel. The separated proteins were transferred to a nitrocellulose membrane, which was then exposed to 5% nonfat dried milk in PBS for 1 h at room temperature before incubation overnight at 4°C with rabbit polyclonal antibodies to human survivin (1:1000 dilution; R&D Systems), to human c-IAP1 (1:1,000 dilution; MBL International), to human XIAP (1:1,000 dilution; Cell Signaling), to human STAT3 (1:1,000 dilution; Cell Signaling), or to β-actin (1:500 dilution; Sigma), or with mouse monoclonal antibodies to human p53 (1:1,000 dilution; Santa Cruz Biotechnology). The membrane was then washed with PBS containing 0.05% Tween 20 before incubation for 1 h at room temperature with horseradish peroxidase–conjugated goat antibodies to rabbit (Sigma) or mouse (Santa Cruz Biotechnology) IgG. Immune complexes were finally detected with chemiluminescence reagents (Perkin-Elmer Life Science).

Clonogenic survival assay. Exponentially growing cells in 25-cm^2 flasks were harvested by exposure to trypsin and counted. They were diluted serially to appropriate densities and plated in triplicate in 25-cm^2 flasks containing 10 mL of complete medium in the presence of 50 nmol/L YM155 or vehicle (final DMSO concentration of 0.1%; we confirmed that this DMSO concentration did not affect the proliferation of NSCLC cell lines). After incubation for 48 h, the cells were exposed at room temperature to various doses of γ-radiation with a ^{60}Co irradiator at a rate of ~0.82 Gy/min. The cells were then washed with PBS, cultured in drug-free medium for 10 to 14 d, fixed with methanol:acetic acid (10:1, v/v), and stained with crystal violet. Colonies containing >50 cells were counted. The surviving fraction was calculated as: (mean number of colonies)/(number of inoculated cells × plating efficiency). Plating efficiency was defined as the mean number of colonies divided by the number of inoculated cells for nonirradiated control cells. The surviving fraction for combined treatment was corrected by that for YM155 treatment alone. Cell survival was corrected according to the equation $S = 1 - (1 - f)^{1/N}$, where S is the single-cell survival rate, f is the measured surviving fraction, and N is multiplicity, which was defined as the average number of cells per microcolony at the time of radiation and which ranged from 2.4 to 6.7 for the cell lines studied under the described conditions. The dose enhancement factor was then calculated as the dose (Gy) of radiation that yielded a surviving fraction of 0.1 for vehicle-treated cells divided by that for YM155-treated cells (after correction for drug toxicity).

Detection of apoptotic cells. Cells were fixed with 4% paraformaldehyde for 1 h at room temperature, after which a minimum of 1,000 cells per sample was evaluated for apoptosis with the use of the terminal deoxynucleotidyl transferase-mediated dUTP nick-end labeling (TUNEL) technique (*In situ* Cell Death Detection Kit; Boehringer Mannheim).

Assay of caspase-3 activity. The activity of caspase-3 in cell lysates was measured with the use of a CCP32/Caspase-3 Fluometric Protease Assay Kit (MBL). Fluorescence attributable to cleavage of the DEVD-AFC substrate was measured at excitation and emission wavelengths of 390 and 460 nm, respectively.

Immunofluorescence staining of γ-H2AX. Cells were grown to 50% confluence in two-well Lab-Tec Chamber Slides (Nunc) and then cultured for 48 h in the presence of 50 nmol/L YM155 or vehicle before exposure to 3 Gy of γ-radiation. At various times thereafter, they were fixed with 4% paraformaldehyde for 10 min at room temperature, permeabilized with 0.1% Triton X-100 for 10 min at 4°C, and exposed to 5% nonfat dried milk for 10 min at room temperature. The slides were washed with PBS and then incubated at room temperature first for 2 h with mouse monoclonal antibodies to histone γ-H2AX (Upstate Biotechnology) at a dilution of 1:300 and then for 1 h with Alexa 488–labeled goat antibodies to mouse IgG (Molecular Probes) at a dilution of 1:700. The slides were mounted in fluorescence mounting medium (Dako Cytomation), and fluorescence signals were visualized with a confocal laser-scanning microscope (Axiovert 200M; Carl Zeiss) equipped with the LSM5 PASCAL system (Carl Zeiss). Three random fields each containing ≈50 cells were examined at a magnification of × 100. Nuclei containing ≥10 immunoreactive foci were counted as positive for γ-H2AX, as previously described (27), and percentage of positive cells was calculated.

Evaluation of tumor growth in vivo. All animal studies were done in accordance with the Recommendations for Handling of Laboratory Animals for Biomedical Research compiled by the Committee on Safety and Ethical Handling Regulations for Laboratory Animal Experiments, Kyoto University. The ethical procedures followed met the requirements of the United Kingdom Coordinating Committee on Cancer Research guidelines (28). Tumor cells (2×10^6) were injected s.c. into the right hind leg of 6-week-old female athymic nude mice (BALB/c nu/nu). Tumor volume was determined from caliper measurement of tumor length (L) and width (W) according to the formula $LW^2/2$. Treatment was initiated when the tumors in each group of animals achieved an average volume of ~200 to 250 mm^3. Treatment groups (each containing eight mice) consisted of vehicle control (physiologic saline), YM155 alone, vehicle plus radiation, and YM155 plus radiation. Vehicle or YM155 at a dose of 5 mg/kg of body mass was administered over 7 consecutive days (days 1-7) with the use of an implanted micro-osmotic pump (Alzet model 1003D; Durect). Mice in the radiation groups received 10 Gy of γ-radiation from a cobalt irradiator either as

a single fraction on day 3 of drug treatment or fractionated over 5 consecutive days (days 3 to 7); the radiation was targeted to the tumor, with the remainder of the body shielded with lead. Growth delay (GD) was calculated as the time required to achieve a 5-fold increase in volume for treated tumors minus that for control tumors. The enhancement factor was then determined as: $(GD_{combination} - GD_{YM155})/GD_{radiation}$.

Statistical analysis. Data are presented as means ± SD or SE and were compared with the unpaired Student's t test. A P value of <0.05 was considered statistically significant.

Results

Inhibition of survivin expression in NSCLC cells by YM155. We first examined the effect of YM155 on survivin expression in human NSCLC cell lines by immunoblot analysis. Treatment of H460 or Calu6 cells with YM155 at 1 to 100 nmol/L for 48 hours inhibited survivin expression in a concentration-dependent manner (Fig. 1A). In contrast, YM155 had no effect on the abundance of other members of the IAP family including XIAP and c-IAP1 (Fig. 1A), suggesting that YM155 specifically inhibits survivin expression in the NSCLC cell lines. The mechanism by which YM155 inhibits survivin expression remains to be elucidated. Previous observations have shown that p53 and signal transducer and activator of transcription 3 (STAT3) regulate survivin expression at the transcriptional level (29). We therefore examined the effect of YM155 on the abundance of p53 and STAT3 in NSCLC cell lines. YM155 showed no marked effect on the amounts of p53 and STAT3 in H460 or Calu6 cells (Fig. 1A), suggesting that the inhibition of survivin expression by YM155 is independent of these transcriptional regulators. Monitoring of the time course of survivin expression in cells exposed to 50 nmol/L

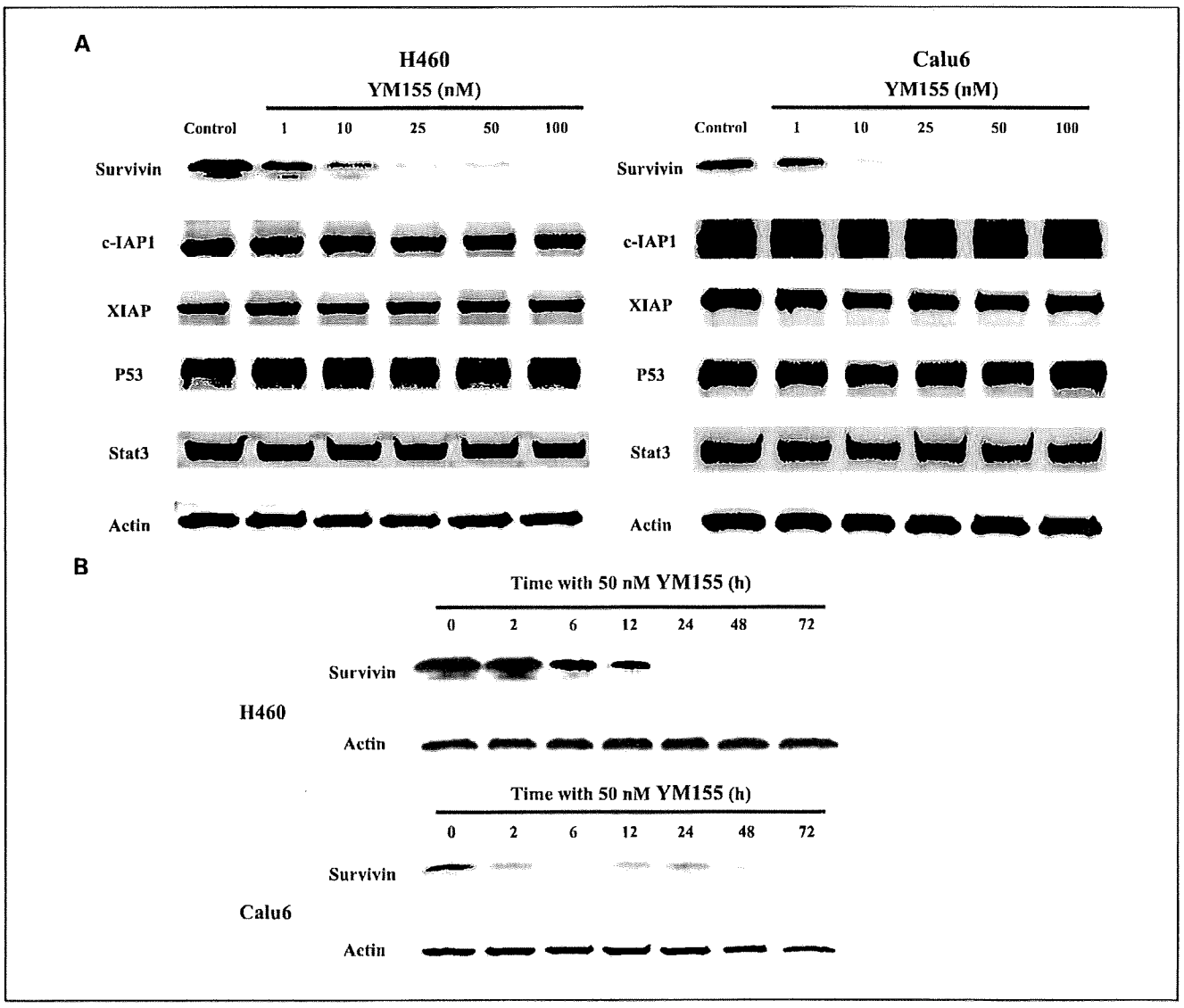

Fig. 1. Effect of YM155 on survivin expression in human NSCLC cells. *A*, H460 or Calu6 cells were incubated in the absence (control, 0.1% DMSO) or presence of various concentrations (1, 10, 25, 50, or 100 nmol/L) of YM155 for 48 h. Cell lysates were then prepared and subjected to immunoblot analysis with antibodies to survivin, to c-IAP1, to XIAP, to p53, to STAT3, or to β-actin (loading control). *B*, H460 or Calu6 cells were incubated with 50 nmol/L YM155 for the indicated times, after which cell lysates were subjected to immunoblot analysis with antibodies to survivin or to β-actin.

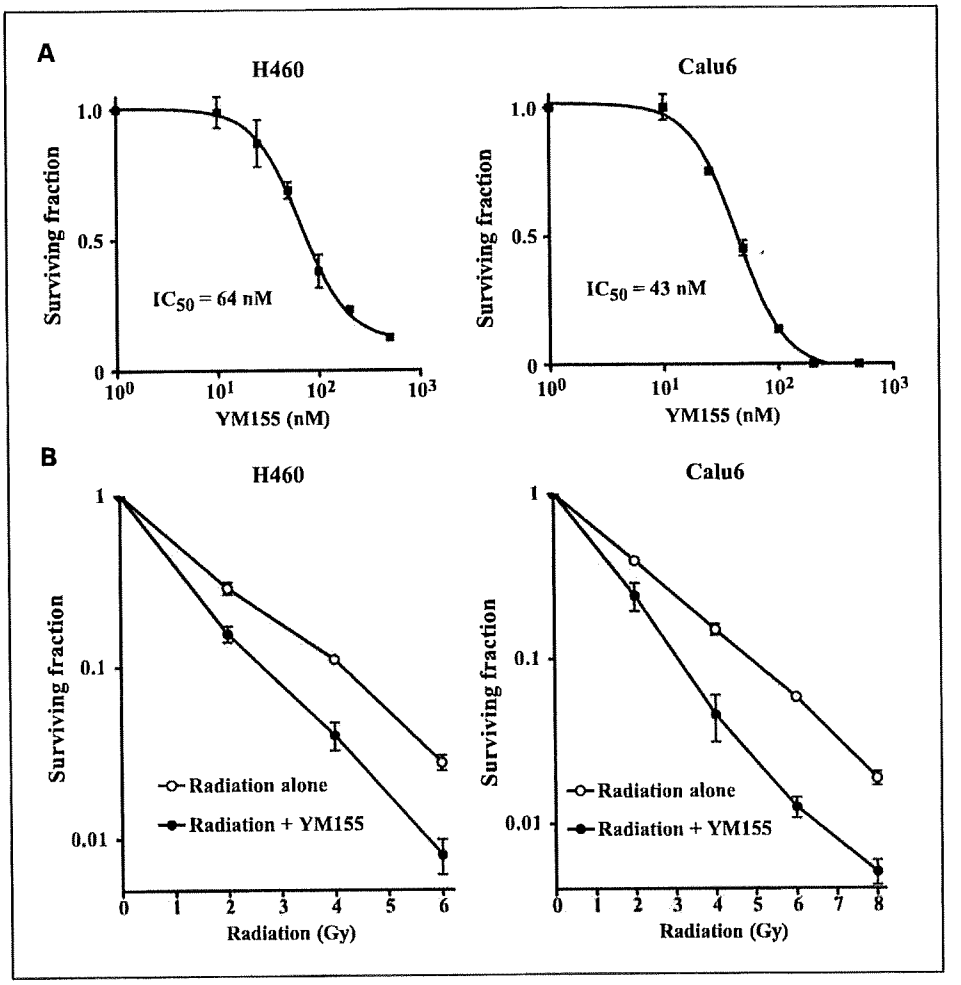

Fig. 2. Effect of YM155 on the sensitivity of H460 or Calu6 cells to γ-radiation. *A*, cells were incubated with the indicated concentrations of YM155 for 48 h and then assayed for clonogenic survival. Points represent means from three independent experiments; bars represent SD. *B*, cells were incubated with 50 nmol/L YM155 or vehicle (control, 0.1% DMSO) for 48 h, exposed to the indicated doses of γ-radiation, and then incubated in drug-free medium for 10 to 14 d for determination of colony-forming ability. Colonies were counted and the surviving fraction was calculated. Plating efficiency for nonirradiated H460 cells was 77.0% and 38.8% for vehicle-treated and YM155-treated cells, respectively; that for nonirradiated Calu6 cells was 57.0% and 23.5%, respectively. All surviving fractions with radiation were corrected for these baseline plating efficiencies. Points represent means from three independent experiments; bars represent SD.

YM155 for up to 72 hours revealed that the abundance of survivin in Calu6 cells had decreased by 2 hours and that survivin was virtually undetectable in H460 cells after 24 hours (Fig. 1B). In both cell lines, treatment with 50 nmol/L YM155 resulted in time-dependent inhibition of survivin expression.

YM155-induced sensitization of NSCLC cells to radiation. To examine the effect of YM155 on cell survival, we first did a clonogenic survival assay. Exposure to the drug at concentrations of 1 to 500 nmol/L for 48 hours revealed that YM155 inhibited the survival of H460 cells with a median inhibitory concentration (IC_{50}) of 64 nmol/L and that of Calu6 cells with an IC_{50} of 43 nmol/L (Fig. 2A). On the basis of these data, we adopted treatment with 50 nmol/L YM155 for 48 hours as the standard protocol for radiation experiments. We next examined whether YM155 might affect the sensitivity of NSCLC cell lines to radiation. Treatment with 50 nmol/L YM155 for 48 hours shifted the survival curves for both H460 and Calu6 cells to the left (Fig. 2B), with a dose enhancement factor of 1.57 and 1.61, respectively, suggesting that YM155 increased the radiosensitivity of both cell lines.

Enhancement of radiation-induced apoptosis in NSCLC cells by YM155. We next examined the effect of YM155 on radiation-induced apoptosis in H460 or Calu6 cells with the use of the TUNEL assay. Combined treatment of either cell line with YM155 and γ-radiation resulted in an increase in the number of apoptotic cells at 24 and 48 hours that was greater than the sum of the increases induced by YM155 or radiation alone (Fig. 3A). To confirm the results of the TUNEL assay, we measured the activity of caspase-3 in cell lysates. Again, the combined treatment of H460 or Calu6 cells with YM155 and γ-radiation induced a synergistic increase in caspase-3 activity (Fig. 3B). These data thus suggested that YM155 promotes radiation-induced apoptosis in NSCLC cell lines.

Inhibition of DNA repair in irradiated NSCLC cells by YM155. Defects in DNA repair have been associated with enhanced sensitivity of cells to radiation (30, 31), and survivin is thought to play a direct or indirect role in DNA repair (21). We therefore next investigated the effect of YM155 on DNA repair by immunostaining of cells with antibodies to the phosphorylated form (γ-H2AX) of histone H2AX, foci of which form at DNA double-strand breaks (DSBs). The formation of γ-H2AX foci in H460 cells was apparent between 30 minutes and 6 hours after γ-irradiation (Fig. 4A). In the presence of YM155, however, these foci persisted for at least 24 hours after irradiation. Evaluation of the percentage of H460 or Calu6 cells with γ-H2AX foci at 24 hours after irradiation revealed that YM155 significantly inhibited the repair of DSBs (Fig. 4B). These results thus suggested that down-regulation of survivin expression by YM155 results in the inhibition of the repair of

radiation-induced DSBs in NSCLC cells, possibly accounting for the observed radiosensitization by this drug.

Enhancement of radiation-induced tumor regression by YM155. To determine whether the YM155-induced radiosensitization of NSCLC cells observed *in vitro* might also be apparent *in vivo*, we injected H460 or Calu6 cells into nude mice to elicit the formation of solid tumors. After tumor formation, the mice were treated with YM155, γ-radiation, or both modalities. YM155 was infused continuously for 7 days with the use of an implanted osmotic pump system, and mice were subjected to local irradiation with a single dose of 10 Gy on day 3 of YM155 administration. Combined treatment with radiation and YM155 inhibited H460 or Calu6 tumor growth to a markedly greater extent than did either modality alone (Fig. 5). The tumor growth delays induced by treatment with radiation alone, YM155 alone, or both YM155 and radiation were 2.9, 5.6, and 14.8 days, respectively, for H460 cells, and 8.9, 41.0, and 76.0 days, respectively, for Calu6 cells. The enhancement factor for the effect of YM155 on the efficacy of radiation was 3.3 for H460 cells and 3.5 for Calu6 cells, revealing the effect to be greater than additive. No pronounced tissue damage or toxicity such as weight loss was observed in mice in any of the four treatment groups.

Finally, we evaluated whether the combination of YM155 and fractionated radiation treatment would result in the inhibition of tumor growth similar to that observed with YM155 plus single-fraction radiation. Mice bearing H460 tumors were thus again subjected to continuous YM155 infusion for 7 days, but local irradiation was done in 2-Gy fractions on days 3 to 7 of drug administration (for a total dose of 10 Gy). The tumor growth delays induced by treatment with radiation alone, YM155 alone, or both YM155 and radiation were 3.8, 5.3, and 16.6 days, respectively (Fig. 6). The enhancement factor for the effect of YM155 on the efficacy of radiation was 3.0. Again, there was no evidence of toxicity on the basis of body weight loss, and there were no animal deaths in any of the four groups. These data suggested that YM155 enhances the tumor response to both single-dose and fractionated radiotherapy *in vivo*.

Discussion

Survivin is a potentially important molecular target for cancer therapy. Reflecting the many mechanisms that seem to regulate survivin expression, diverse approaches have been evaluated for targeting survivin in experimental models. Although certain drugs, such as inhibitors of histone deacetylases,

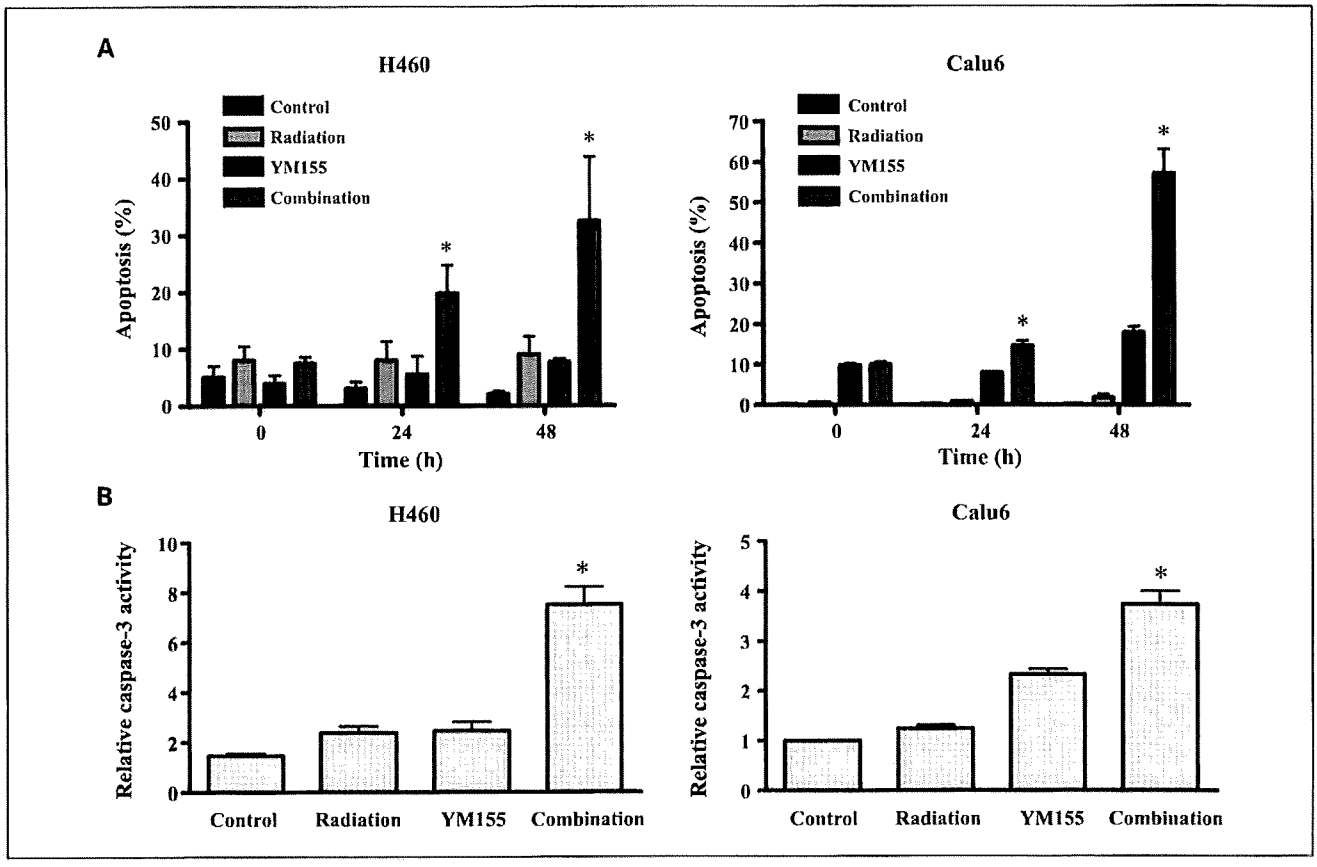

Fig. 3. Effect of YM155 on radiation-induced apoptosis and caspase-3 activity in H460 or Calu6 cells. *A*, cells were incubated with 50 nmol/L YM155 or vehicle (0.1% DMSO) for 48 h, exposed (or not) to 3 Gy of γ-radiation, and then incubated in drug-free medium for 24 or 48 h, at which times the percentage of apoptotic cells was determined by TUNEL staining. *B*, lysates of cells treated as in *A* were assayed for caspase-3 activity 24 h after irradiation. Columns represent means from three independent experiments; bars represent SD; those in *B* are expressed relative to the corresponding value for the control condition. * $P < 0.01$ versus the corresponding value for treatment with radiation or YM155 alone.

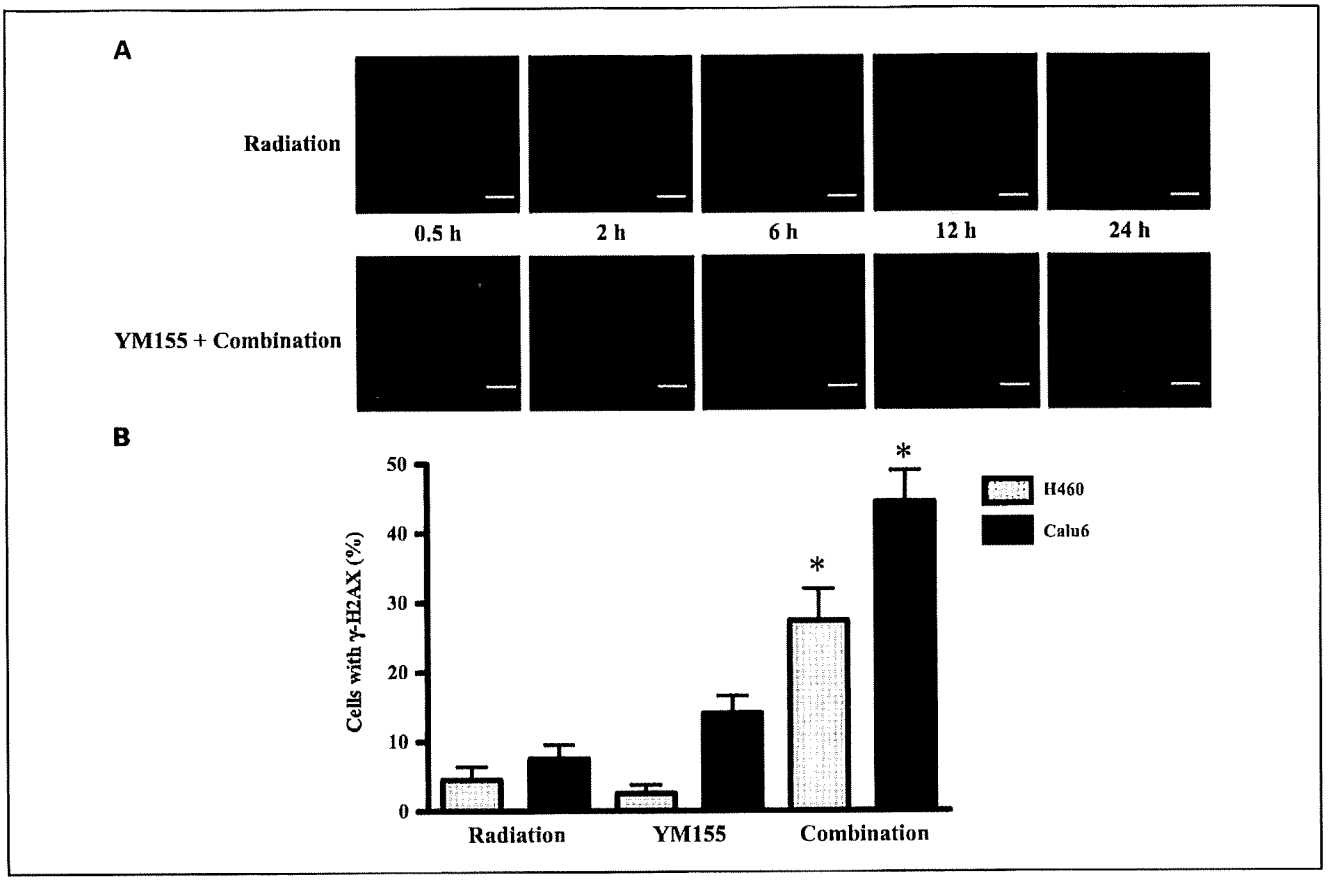

Fig. 4. Effect of YM155 on the radiation-induced formation of γ-H2AX foci in NSCLC cells. *A*, H460 cells were incubated with vehicle (0.1% DMSO) or 50 nmol/L YM155 for 48 h and then exposed to 3 Gy of γ-radiation. After incubation for the indicated times in drug-free medium, the cells were fixed and subjected to immunofluorescence staining for γ-H2AX (green fluorescence). Scale bar, 10 μm. *B*, H460 or Calu6 cells were incubated with vehicle or YM155 and then exposed (or not) to γ-radiation as in *A*. They were fixed at 24 h after irradiation and the percentage of cells containing γ-H2AX foci was determined. Columns represent means from three independent experiments; bars represent SD. $^*P < 0.05$ versus the corresponding value for radiation or YM155 alone.

mitogen-activated protein kinases, and cyclin-dependent kinases, have been shown to suppress survivin expression by targeting various signaling pathways, these drugs inhibit survivin expression nonspecifically (15–17, 19, 32). Gene therapy strategies based on small interfering RNA or other antisense oligonucleotides are specific for survivin, but the effective delivery of these molecules remains a challenge for the transition to the clinic (33). YM155 is a small-molecule agent that specifically inhibits survivin expression in various types of cancer cell lines *in vitro* (14). In addition, YM155 has been shown both to distribute preferentially to tumor tissues rather than to plasma as well as to exert pronounced antitumor activity in tumor xenograft models *in vivo* (14). The use of YM155 as a single agent in phase I clinical trials did not reveal significant toxicity (34). Although phase II studies of YM155 use as a single agent for certain types of cancer are currently under way, the effects of YM155 in combination with radiation have not been reported. We now show that YM155 increased the sensitivity of tumor cells to radiation *in vitro* and *in vivo*.

Clonogenic survival analysis, the most reliable approach for assessing the ability of genotoxic agents to induce cell death (35), revealed that YM155 markedly potentiated the decrease in NSCLC cell survival induced by γ-radiation. Given that induction of apoptosis is a key mechanism of cytotoxicity for most antitumor agents, including γ-radiation, defects in apoptotic signaling may underlie resistance to such agents (36). Radiation-sensitive tumors undergo radiation-induced apoptosis *in vitro* more readily than do radiation-resistant tumors (37–40). Treatment with caspase inhibitors has been shown to protect tumor cells against radiation-induced apoptosis and to increase their radioresistance (21, 41, 42), suggesting that radiation-induced apoptosis is caspase-dependent and that caspases contribute to radiosensitivity. The antiapoptotic activity of survivin is mostly attributable to inhibition of the activation of downstream effectors of apoptosis such as caspase-3 and caspase-7 (25). We have now shown that radiosensitization of NSCLC cells by YM155 was associated with increases both in the activity of caspase-3 and in the proportion of apoptotic cells. Our findings thus suggest that YM155 sensitized tumor cells to radiation at least in part by enhancing radiation-induced apoptosis.

We examined further the mechanism by which YM155 induces radiosensitization. Survivin is essential for the proper execution of mitosis and cell division, with disruption of survivin expression resulting in cell division defects that can lead to polyploidy and the formation of multinucleated cells (43, 44). Although treatment with 50 nmol/L YM155 for 48 hours inhibited survivin expression in NSCLC cells, it